Australian Government
Department of Defence
Defence Science and
Technology Organisation

On Alternative Formulations for Linearised Miss Distance Analysis

Domenic Bucco and Rick Gorecki

Weapons Systems Division
Defence Science and Technology Organisation

DSTO-TR-2845

ABSTRACT

In this report, techniques generally employed in the analysis of intercept guidance problems are reviewed. From the governing non-linear equations describing such problems, two basic linear models are derived. Traditionally, these linear models are utilised as a basis for preliminary intercept engagement studies. Under certain input conditions, the two models are mathematically equivalent and, hence, have been used interchangeably by weapons analysts to yield appropriate design and performance data in support of their programs. However, for a specific set of initial conditions, which includes a very important class of practical problems that may be assessed with the use of these models, it is noted herein that one of these linear models produces incorrect performance data when compared to a non-linear simulation of the engagement. In contrast, the other model produces consistent results with those generated by the non-linear simulation regardless of the initial conditions considered. To remedy this discrepancy, the necessary mathematics are derived to bring the two formulations into alignment for any form of the initial conditions and inputs to the system. Consequently, this leads to a consistency in the corresponding adjoint models which are constructed from these linear models, thus ensuring the generation of correct output data regardless of which model is employed by the analyst.

Published by

Weapons Systems Division
DSTO Defence Science and Technology Organisation
PO Box 1500
Edinburgh South Australia 5111 Australia

Telephone: 1300 DEFENCE
Fax: (08) 7389 6567

AR-015-622
May 2013

APPROVED FOR PUBLIC RELEASE

On Alternative Formulations for Linearised Miss Distance Analysis

Executive Summary

In this report, the missile-target engagement problem is analysed. As part of the analysis, the non-linear governing equations are reviewed for motion in a single plane. These non-linear equations are employed for two purposes. Firstly, the equations form the basis of a non-linear simulation program developed in Simulink. This Simulink model is controlled and executed via a graphical user interface specifically developed as an aid for the weapons analyst to study the engagement problem. Secondly, the non-linear equations are utilised as a basis for linearisation and, hence, the derivation of an approximate linear model of the engagement. Two different formulations of the linear model are derived. These are designated as Model A and Model B in the report.

Although both models are generally used interchangeably in the literature for guided missile homing loop analysis, it is demonstrated herein that, under certain input conditions, care needs to be exercised when using one of these models, Model A, for performance analysis. In order to ensure that both models yield the same performance data for all input conditions considered, a correction factor is derived. This correction factor needs to be included in the form of an added initial condition on one of the states in the state space representation of Model A. Simulation results show that the two models are in agreement when this correction factor is applied. Knowledge of this fact is important to ensure that analysts generate correct performance data when using linear techniques such as the adjoint method. The adjoint model is constructed from a knowledge of the forward linear model, that is, Model A or Model B, and is traditionally employed by analysts as part of the solution process.

To gain further insight into the nature of the missile-target engagement problem and the parameters that influence performance, also included in this report is an analytical treatment of the problem. It is well known that, when the missile guidance dynamics is represented by a first order lag (single time constant system), then the linear differential equations describing the intercept problem are readily amenable to analytical treatment. Consequently, an analytical investigation of each model (A and B) is carried out for the range of input conditions considered herein. The resulting closed form solutions from each model are compared and are shown to be mathematically equivalent for all input conditions considered provided that Model A has the proposed correction factor implemented. For simulation purposes, the corresponding adjoint model of Model A and Model B are constructed and then implemented in Simulink. As with the analytical results, outputs from the two models are shown to be in agreement. Finally, the models are extended to represent more realistic guidance system dynamics (fifth order system) and simulation results are generated and compared.

Finally, a special relationship linking two of the derived miss distance formulas is noted and explored further. This relationship highlights a connection between the miss distance due to an initial target displacement and that due to an initial heading error in the context of the linear analysis. Following verification using linear simulation, a formula based on this relationship is derived and proposed as a means for predicting performance data of more complex linear systems. This formula may also be used in connection with the non-linear simulation model for generating approximate miss distance profiles due to the effects of a step in target position prior to intercept. A step in target position typically arises in problems associated with the seeker resolution of the target in a multi-target scenario. It may also arise in the case of a single target scenario. For this case, the missile may be on a collision course with the predicted intercept point (PIP) of the target. However, at the time of seeker turn-on, the PIP may not necessarily coincide with the actual target position.

Authors

Domenic Bucco
Weapons Systems Division

Domenic Bucco received his PhD in Applied Mathematics from the University of Adelaide, South Australia.

Since 1980, he has been working at the Defence Science and Technology Organization (DSTO) in Australia as a research scientist in the Weapons Systems Division. He has worked in various areas of the division including guidance and control, modelling and simulation, hardware in the loop and weapon robotics.

During 1987/1988, he was posted to the Naval Air Warfare Centre, China Lake, California, as an exchange scientist for 18 months. While there, he worked on autopilot design and hardware-in-the-loop simulations.

During 2008/2009, he was awarded a Defence Fellowship to conduct research on the aerospace applications of adjoint theory.

He is currently working as a principal research scientist supporting Guidance and Control research in the Division.

Rick Gorecki
DSTO

Mr Richard Gorecki was awarded a B Tech in Electronic Engineering at Adelaide University and a Graduate Diploma in Mathematics at the University of South Australia. During his time at the Defence Science and Technology Organisation (DSTO) in Australia he worked mostly on missile modelling and simulation including six degrees of freedom (6DOF) models of most of the missiles in the ADF inventory. He also spent some time in ship Radar signature measurement and modelling and Optical and IR sensor modelling and analysis of C3I systems. In later years he developed a model of a hardware in the loop (HWIL) facility.

Since his retirement from DSTO he has worked for Daintree Systems on contracts involving towed target attrition, HWIL simulation of two target scenarios and 6DOF missile simulation models.

Contents

1. Introduction

The equations describing the dynamics and geometrical interactions between an interceptor and its target are generally non-linear and complex and are usually beyond the scope of analytical investigations. Therefore, they are solved approximately using computer simulation. Simulation provides the missile analyst with a basic capability for assessing the performance and behaviour of the interceptor under varying conditions of the engagement and can provide answers to questions such as, "What is the overall effect on miss distance due to a sudden shift in target direction?" However, to gain critical insight into the nature of such interactions and to identify key parameters that may affect the performance and behaviour of the interceptor, engineers often make use of simplifying assumptions in order to linearise the governing equations. Once in linear form, the engagement equations are more easily tackled using established linear techniques. Two such techniques are the adjoint simulation method and the covariance analysis method.

In this report, we first review the engagement model based on two dimensional (2D) non-linear dynamics. Following this, we make use of linearisation to reduce the equations to a form amenable to linear analysis. Using standard block diagram algebra, these linear equations are then used to derive two basic models, referred to as Model A and Model B, which may be used as the basis for the linear analysis of planar missile/target engagements. In the literature, these models are often used interchangeably for preliminary analysis of the performance of guided missile systems [1-6]. However, as is demonstrated herein, caution must be used when adopting one of these models under certain initial conditions of the state variables. It is shown that the mathematical equivalence of the two block diagram topologies representing the models is dependent on the nature of the initial conditions imposed on the states of the system. For example, if the initial condition is based on an initial heading error in the missile, then both models yield the same miss distance results. However, if the initial condition stems from a step in target displacement (this condition is used to study missile performance against multiple targets), then the two block diagram topologies, as currently employed in the open literature, will lead to miss distance results that differ significantly. Consequently, applying the adjoint method to these two systems will also give different results. To correct this inconsistency, the necessary mathematics is derived to bring the two formulations into alignment for any of the initial state conditions. This then leads to consistency in the associated adjoint models regardless of which linear formulation is pursued by the analyst. In addition, closed form solutions of the miss distance variation in terms of flight time have been derived for the case when the missile guidance loop may be approximated dynamically by a first order lag term. Finally, simulation results and design curves are generated for more realistic guidance systems.

2. Non-linear Engagement Equations

2.1 Planar Engagement Model

Consider a missile-target engagement under the following assumptions; the engagement is confined to the X-Y plane, the force due to gravity is ignored, and the missile velocity and the target velocity remain constant. The geometry of the engagement is depicted in Figure 1.

The non-linear differential equations describing the motion of the target are [1],

$$\dot{X}_T = -V_T \cos(\beta) \tag{1}$$

$$\dot{Y}_T = V_T \sin(\beta) \tag{2}$$

$$\dot{\beta} = \frac{n_T}{V_T} \tag{3}$$

where (X_T, Y_T) defines the target position, V_T is the constant target speed, n_T is the target acceleration while β refers to the target flight path angle as shown in Figure 1. The dots over the variables denote differentiation with time. The initial conditions are given by $X_T(0) = X_{T0}$, $Y_T(0) = Y_{T0}$ and $\beta(0) = \beta_0$.

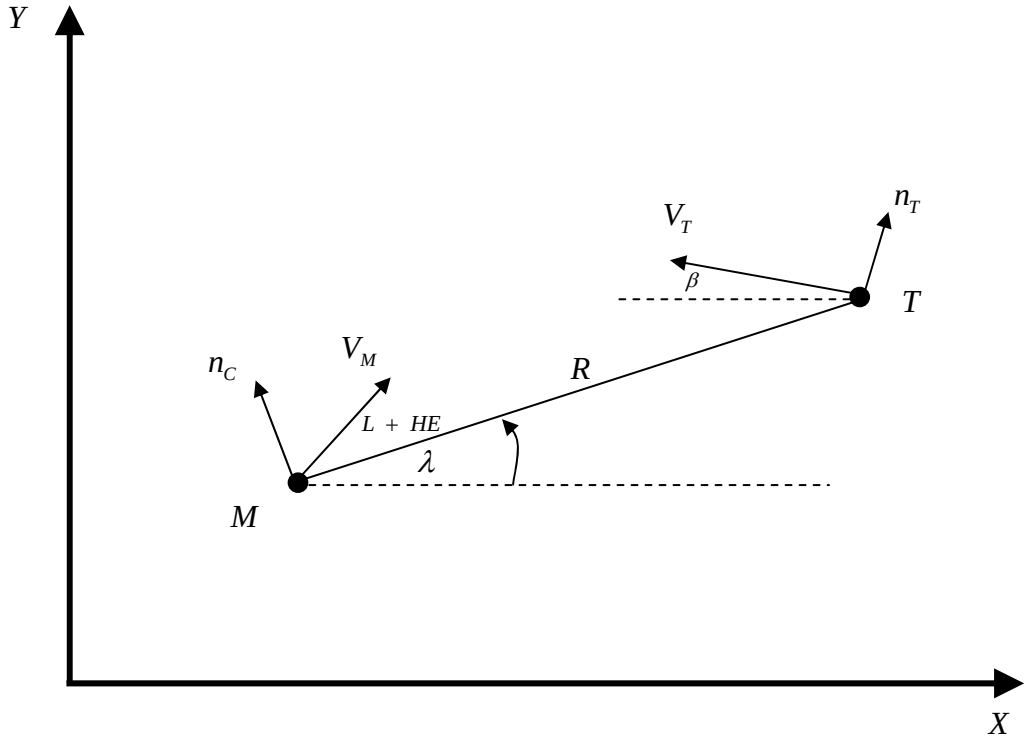

Figure 1. Engagement Geometry

Similarly, the non-linear differential equations describing the motion of the missile are,

$$\dot{X}_M = V_{MX} \tag{4}$$

$$\dot{Y}_M = V_{MY} \tag{5}$$

$$\dot{V}_{MX} = -n_c \sin(\lambda) \tag{6}$$

$$\dot{V}_{MY} = n_c \cos(\lambda) \tag{7}$$

Here, (X_M, Y_M) defines the instantaneous position of the missile while (V_{MX}, V_{MY}) are the components of its velocity vector. Furthermore, n_c denotes the missile commanded acceleration and λ is the line of sight angle as shown in Figure 1. The initial conditions are given by $X_M(0) = X_{M0}$, $Y_M(0) = Y_{M0}$, $V_{MX}(0) = V_M \cos(L + HE + \lambda)$ and $V_{MY}(0) = V_M \sin(L + HE + \lambda)$ where V_M denotes the constant missile speed, L is the missile lead angle associated with the collision triangle and HE refers to the initial deviation of the missile from the collision triangle commonly known as the heading error. The lead angle L can be found by application of the law of sines on the collision triangle yielding the formula

$$L = \sin^{-1}\{V_T \sin(\beta + \lambda)/V_M\}\,. \tag{8}$$

To find the missile acceleration components, it is necessary to determine the components of the relative missile-target separation. Let the components of the relative missile-target separation be expressed as

$$\Delta_X = X_T - X_M\,, \tag{9}$$

$$\Delta_Y = Y_T - Y_M\,. \tag{10}$$

Consequently, the range R between missile and target is given by

$$R = (\Delta_x^2 + \Delta_y^2)^{\frac{1}{2}}\,, \tag{11}$$

while the line of sight angle λ is given by

$$\lambda = \tan^{-1}\left(\frac{\Delta_Y}{\Delta_X}\right). \tag{12}$$

The line of sight rate can be easily derived from this expression by differentiating with respect to time, giving

$$\dot{\lambda} = \frac{\Delta_X \dot{\Delta}_Y - \dot{\Delta}_X \Delta_Y}{R^2}. \tag{13}$$

The closing velocity is defined as the negative rate of change of the missile target separation, that is, $V_c = -\dot{R}$, which, after using eq (11) above, leads to the relation,

$$V_C = \frac{-(\Delta_X \dot{\Delta}_X + \Delta_Y \dot{\Delta}_Y)}{R}. \tag{14}$$

Consequently, the magnitude of the missile guidance command n_C can be found from the definition for proportional navigation guidance,

$$n_C = N' V_c \dot{\lambda}, \tag{15}$$

where N' is a given constant.

If we model the actual acceleration of the missile n_L by a first order lag term, then

$$\frac{n_L}{n_C} = \frac{1}{1+\tau s}. \tag{16}$$

A 2D simulation model is easily developed using the above equations. For this study, MATLAB/Simulink was used to develop the simulation model. The top level Simulink model is presented in Figure 2. The details of each subsystem of the model are given in Appendix A. Figure 3 presents a screen shot of the Graphical User Interface (GUI) used in this study. The GUI was specifically designed as an aid in running the simulation. The MATLAB software underpinning the construction of the GUI is also presented in the Appendix.

At the GUI level, the missile and target parameters may be entered by the analyst. On the left of the GUI, the analyst can enter initial target position, target speed and flight path angle. On the right of the GUI, the analyst can enter initial missile position, missile speed, effective navigation constant and guidance loop time constant. Inputs for the simulation include target manoeuvre (NT), error in the initial heading angle (HE) and jump in the target position (Displace) at some time (THOM) prior to intercept.

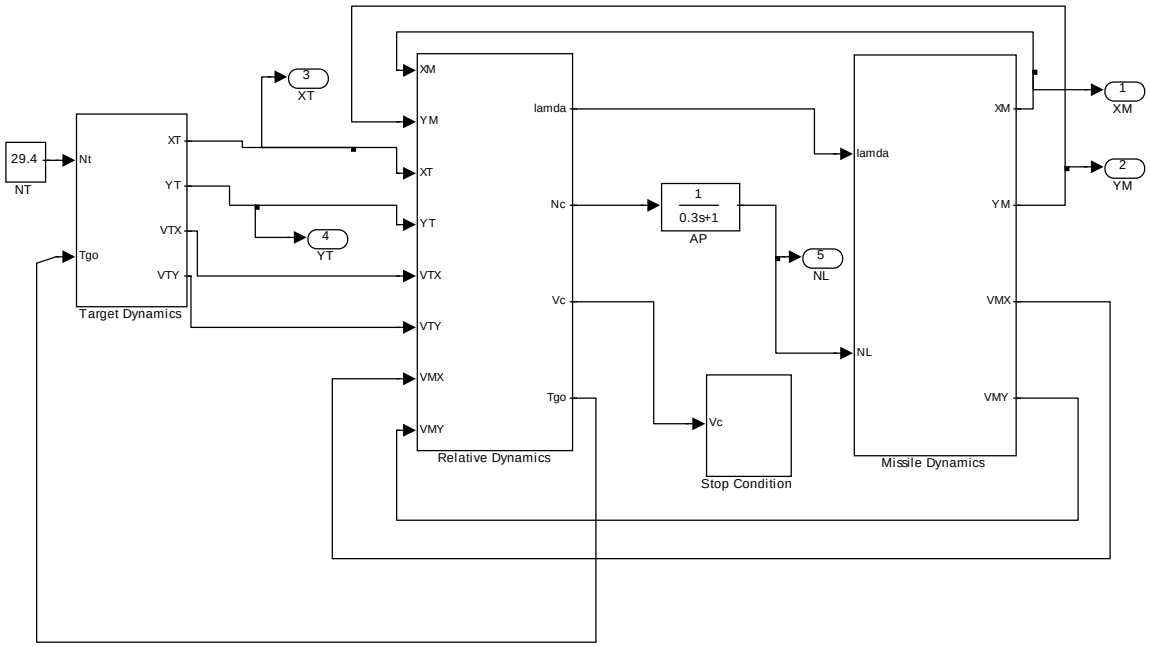

Figure 2 Two Dimensional Engagement Model in Simulink

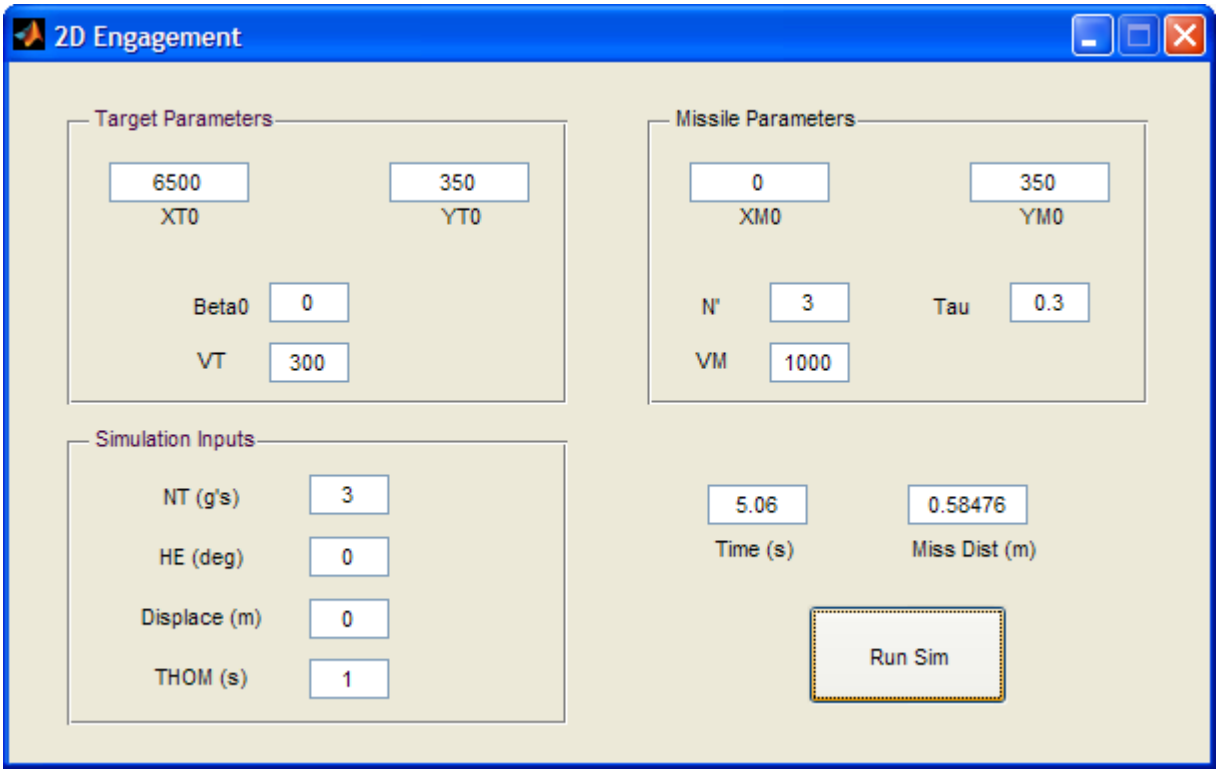

Figure 3. Graphical User Interface to run the 2D Engagement Model

2.2 Simulation Results

The Simulink model given above may now be used to conduct simulation studies of the missile/target engagement problem. The simulation studies will be based on the following three simulation inputs;

(a) a step in target manoeuvre
(b) an error in initial heading angle
(c) a step in target position

Interest in (c) above stems from the analysis of multi-target scenarios as is described in Section 2.2.3.

2.2.1 Step in target manoeuvre

Consider the case in which the only disturbance is a $3g$ target manoeuvre starting at time $t = 0$. The nominal values for target and missile parameters may be easily identified in the GUI given in Figure 3. In this scenario, the missile and target are initially on a collision course and flying along the downrange component of the earth fixed co-ordinate system. Thus, the target velocity vector is initially along the line of sight and, at first, all $3g$ of the target acceleration are perpendicular to the line of sight. However, as the target manoeuvres, the magnitude of the target acceleration perpendicular to the line of sight reduces due to the turning of the target.

Sample missile/target trajectories for this case with effective navigation ratios of 3 and 5 are shown in Figure 4. It is clear from the figure that the higher effective navigation ratio causes the missile to lead the target slightly more than the lower navigation ratio case.

Figure 5 presents the respective missile acceleration profiles obtained from the simulations. Note that, although both acceleration profiles are monotonically increasing for most of the flight, the higher effective navigation ratio case leads to less acceleration requirement of the missile towards the end of flight. Also noteworthy from the plot is the observation that the peak acceleration required by the missile to hit the target is significantly higher than the manoeuvre level of the target ($3g$).

2.2.2 Heading error

Next, consider the case in which the only disturbance is a 20 degree error in the initial heading angle, that is, HE = -20 deg. Again the simulation was run for two values of the effective navigation ratio. Sample trajectories for effective navigation ratios of 3 and 5 are presented in Figure 6. From the figure, it is apparent that initially the missile is flying in the wrong direction because of the heading error. Gradually the guidance law forces the missile to head towards the target. It is interesting to note from the figure that the larger effective navigation ratio enables the missile to remove the initial heading error more rapidly, thus leading to a tighter missile trajectory in this case.

In Figure 7 is plotted the resultant missile acceleration profiles for each case. From the figure, it is observed that the faster removal of heading error in the higher effective navigation ratio case is associated with larger missile accelerations at the beginning of flight

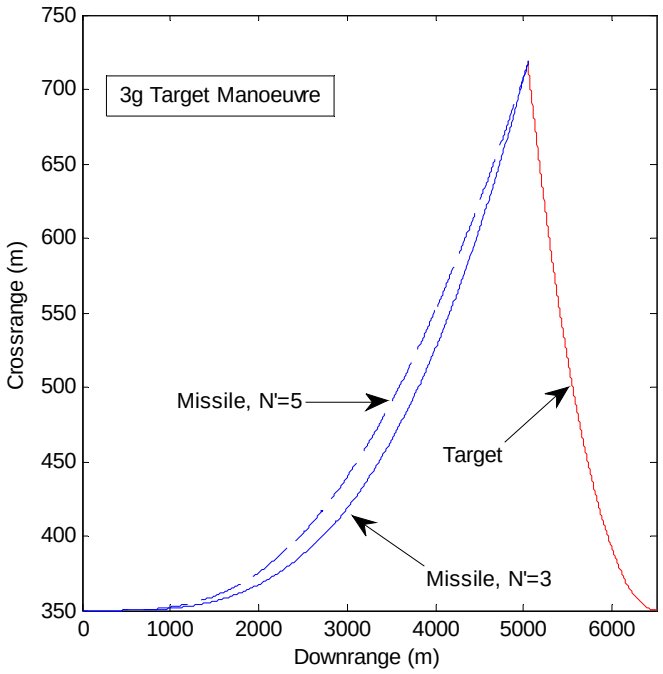

Figure 4: Missile performance against manoeuvring target

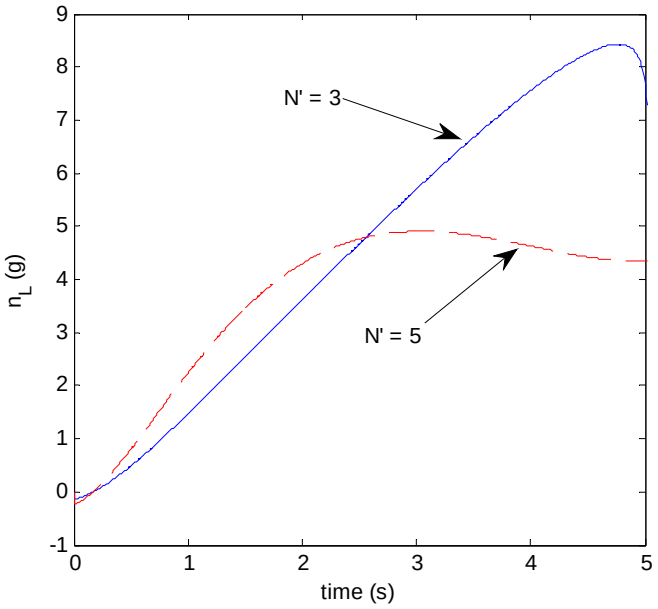

Figure 5: Acceleration profile for Target Manoeuvre Case

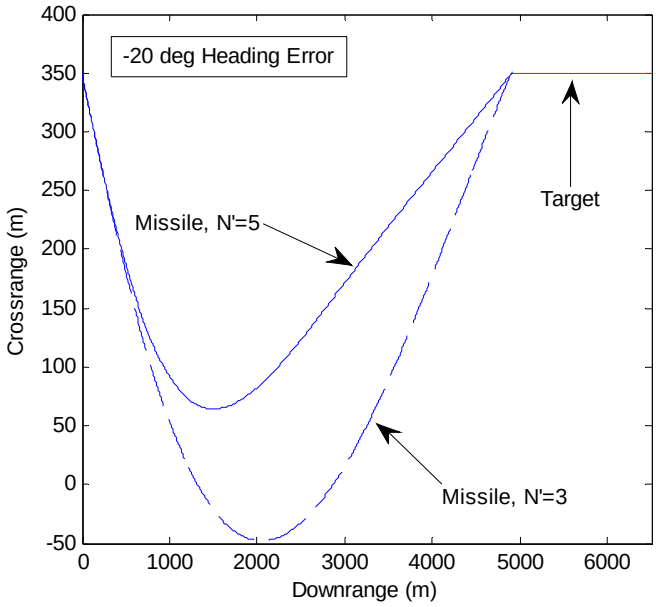

Figure 6: Missile performance when initial heading angle is in error

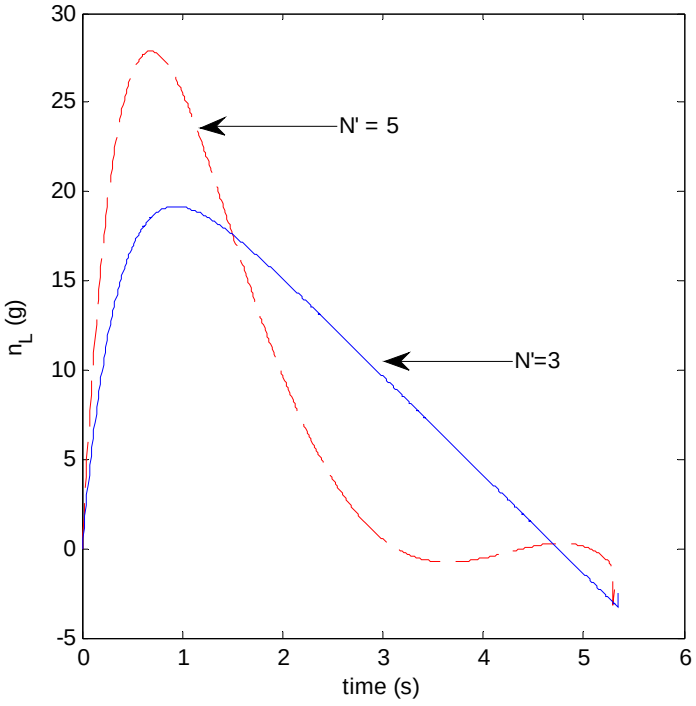

Figure 7: Missile performance when initial heading angle is in error

2.2.3 Step in target position

The non-linear engagement simulation program may be used to analyse the missile response to a sudden jump in target position at a certain time prior to intercept. This is useful in supporting simulation studies concerning the effects of seeker resolution on the performance of the missile when confronted with multiple targets.

Consider the scenario shown in Figure 8 [1]. On the left is the missile engaging two targets which are flying in formation. Both targets have the same speed and are separated by a spacing of Δd metres. It is assumed here that the power centroid is located half way between the targets. In this case, the input parameter, "Displace" in the GUI of Figure 3 is equivalent to $\Delta d / 2$ metres. For the simulation, it is assumed that the missile is initially on a collision course with the power centroid. At a certain time to go before intercept with the power centroid, seeker resolution occurs and the missile is presented with the true target, that is, Target 1. At this time, it will appear to the missile as if the target position jumps from the power centroid to Target 1. From a simulation perspective, it is only necessary to model the target currently seen by the missile. Therefore, for most of the flight, the missile will be guiding on the power centroid and for the rest of the flight, following seeker resolution, the missile will be guiding on Target 1. This is represented in the simulation by the target position being updated by a step in target displacement at a given time to go prior to intercept (THOM).

The non-linear 2D engagement model is used to generate sample simulation results of this type of engagement. Relevant simulation results are presented in Figure 9 and 10 below.

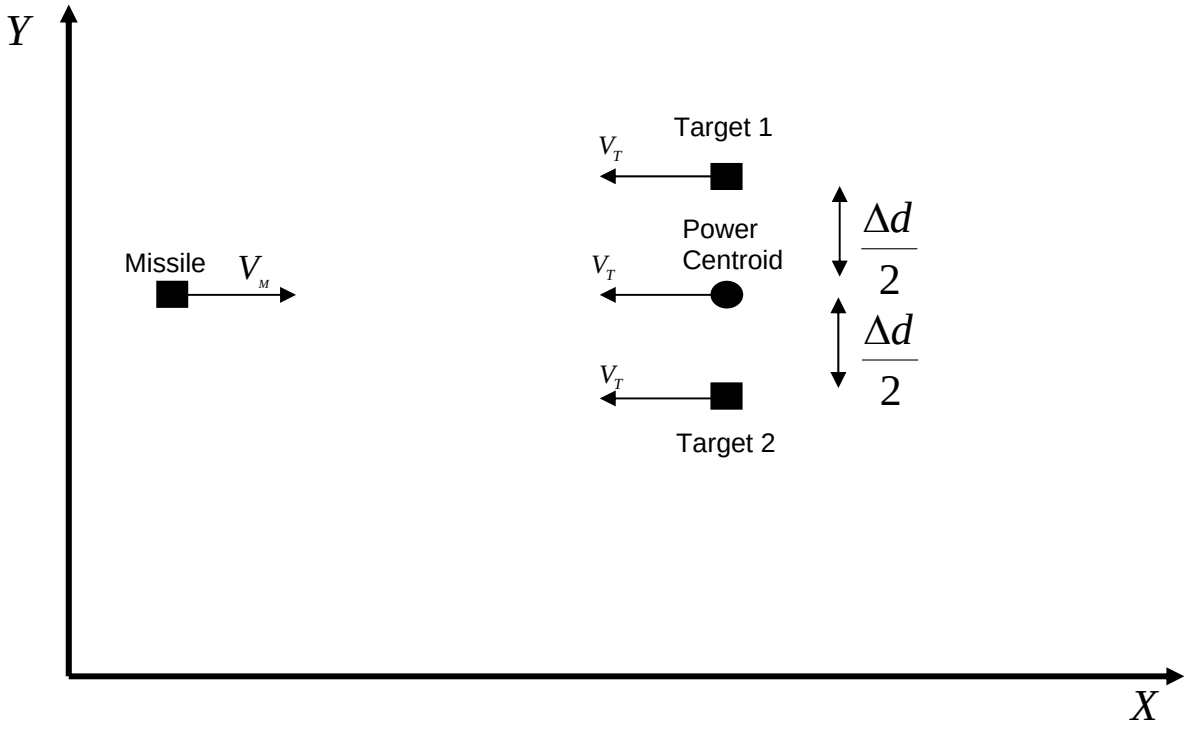

Figure 8: Missile engaging two targets flying in formation

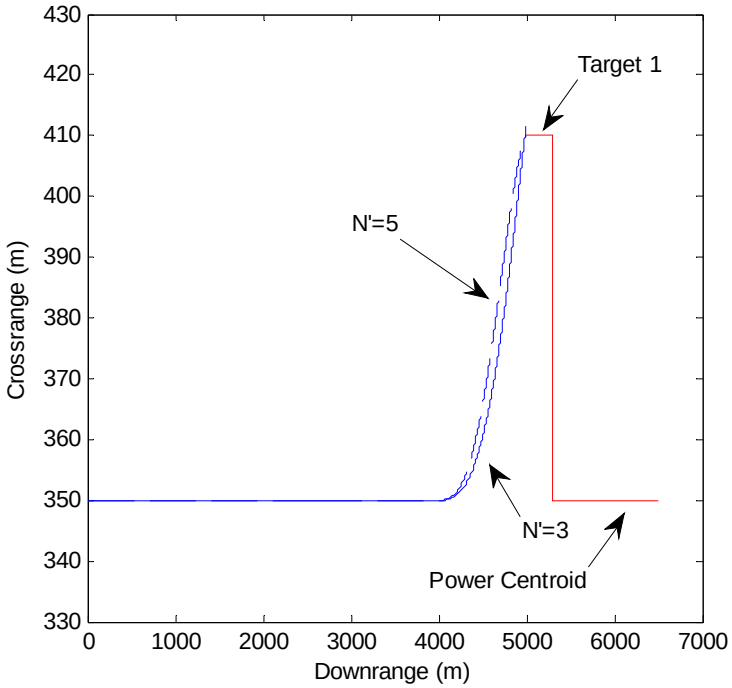

Figure 9: Missile performance in multi-target case

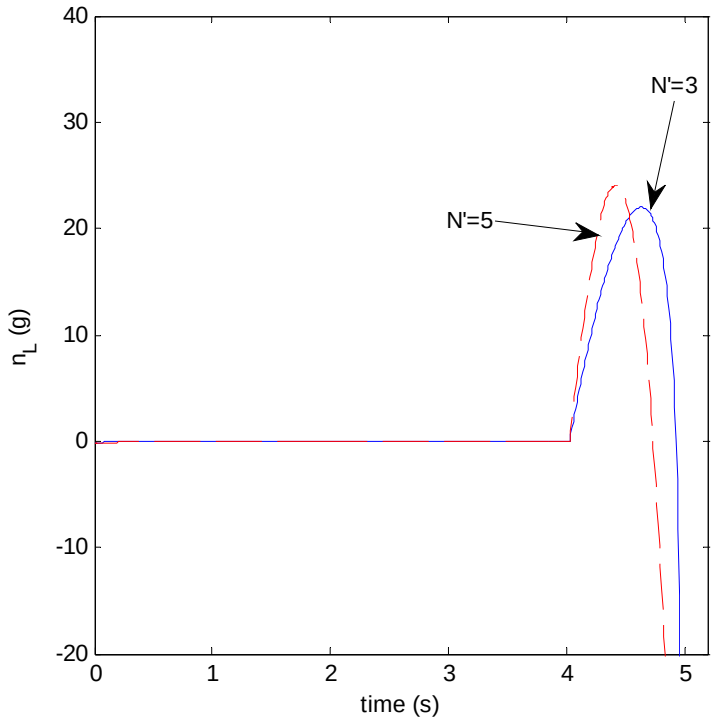

Figure 10: Acceleration profile in multi-target case

3. Linearised Engagement Equations

In this section, analytical tools are employed to gain further insight into the performance of the interceptor under different engagement conditions and to better understand its dynamic response. In particular, the adjoint method is applied to a simplified version of the engagement equations. The simplified equations of motion are derived using linearization about the line of sight angle between missile and target. The procedure follows closely that outlined in Zarchan [1].

First, define the relative separation between the missile and target perpendicular to the fixed reference as defined in Figure 11,

$$y = Y_T - Y_M \ . \tag{17}$$

The relative acceleration is expressed, by inspection of the figure, as

$$\ddot{y} = n_T \cos\beta - n_C \cos\lambda \ . \tag{18}$$

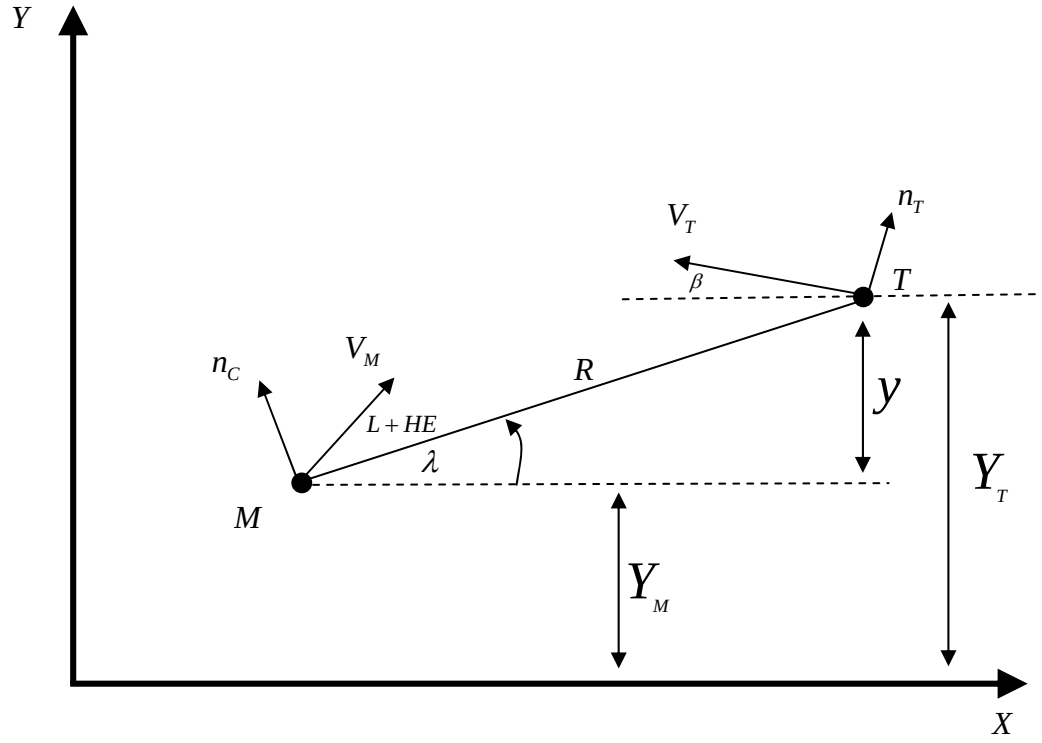

Figure 11: Engagement Geometry for Linearisation

For small flight path angles, that is, near head-on or tail chase case, the cosine terms are approximately unity, and the previous equation (18), reduces to

$$\ddot{y} = n_T - n_C \ . \tag{19}$$

Similarly, the line of sight angle, which is given by,

$$\sin\lambda = \frac{y}{R}, \tag{20}$$

may also be linearised, using the small angle approximation, yielding the expression

$$\lambda = \frac{y}{R}. \tag{21}$$

For a head-on case, the closing velocity is approximated by

$$V_C = V_M + V_T, \tag{22}$$

and in a tail chase situation, the closing velocity is approximated by

$$V_C = V_M - V_T. \tag{23}$$

Consequently, for constant missile and target speed, the closing velocity may be treated as a positive constant. However, the closing velocity has previously been defined as the negative derivative of the range from missile to target, that is, $V_c = -\dot{R}$, and since the range must go to zero at the end of flight, we can approximate the range equation with the time varying relationship,

$$R = V_C(t_F - t). \tag{24}$$

In the above expression, t denotes the current time and t_F is the total flight time of the engagement. Note that t_F is a constant here.

The linearised miss distance is defined to be the relative separation between missile and target at the end of flight, namely,

$$MD = y(t_F). \tag{25}$$

Using equations (19), (21), (24) and (25), and adding the information given by equations (15) and (16), we are able to build a block diagram model for the linearised version of the homing equations. This model is displayed in Figure 12 below. In the diagram, the symbol s refers to differentiation in the frequency domain using Laplace Transform terminology.

In order to implement this block diagram model in Simulink, it is prudent to combine the single s block with the transfer function block given by $1/(1+\tau s)$. This is possible in this case as $N'V_C$ is a constant. Thus, following this process, the revised block diagram model for the linearised equations is presented in Figure 13. This model is designated here as Model A. Note

that the block diagram displayed in Figure 13 now contains an inner closed loop block structure. This alternative block structure is mathematically equivalent to the single block with transfer function $s/(1+\tau s)$. The process is known as reducing the block to its fundamental closed loop form and has been achieved here using standard block diagram algebra. This alternative representation is important in the sequel.

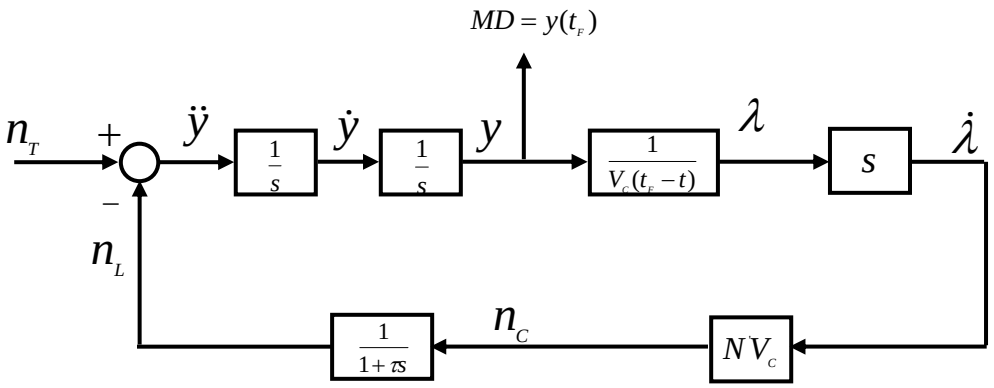

Figure 12: Linearised Geometry Model

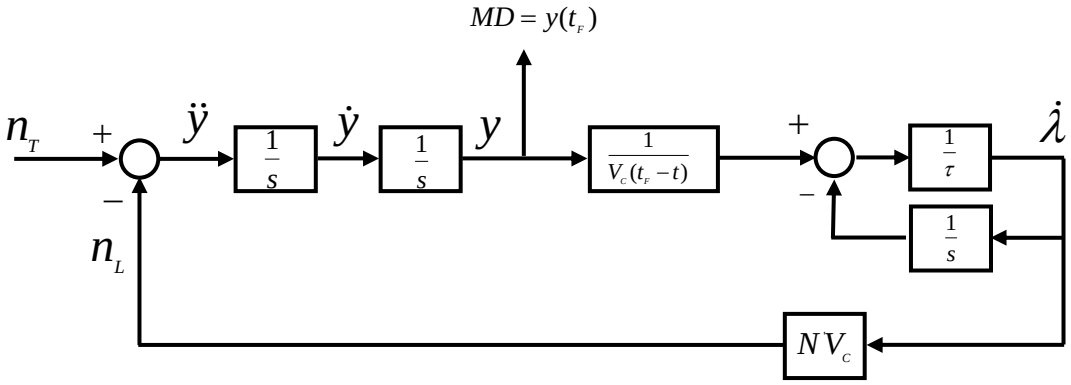

Figure 13: Linear Model A

Model A is typically employed in support of analytical studies of the homing loop problem in the literature [1,2,3]. This model is also used as the basis for adjoint analysis of the guidance loop. It is shown in the sequel that while this model is useful for performance studies associated with target manoeuvre and heading error effects, caution needs to be exercised when using the model as a basis for analysis of multi-target problems.

An alternative block diagram structure typically employed in the literature for homing loop studies [1,4,5,6] may be derived using the analytical expression for the rate of change of line of sight angle. For the non-linear model, the rate of change of the line of sight angle is given in equation (13). After applying the linearisation conditions stipulated above, the expression for the line of sight rate becomes

$$\dot{\lambda} = \frac{\dot{y}}{V_C(t_F - t)} + \frac{y}{V_C(t_F - t)^2}, \tag{26}$$

or equivalently,

$$\dot{\lambda} = \frac{(t_{go}\dot{y} + y)}{V_C t_{go}^2}, \tag{27}$$

where the term t_{go} denotes the time to go and is defined as $t_{go} = t_F - t$.

After incorporating the analytical expression for the line of sight rate into the linearised set of equations, an alternative block diagram for the homing loop dynamics may be derived. This alternative block diagram, designated as Model B, is displayed in Figure 14.

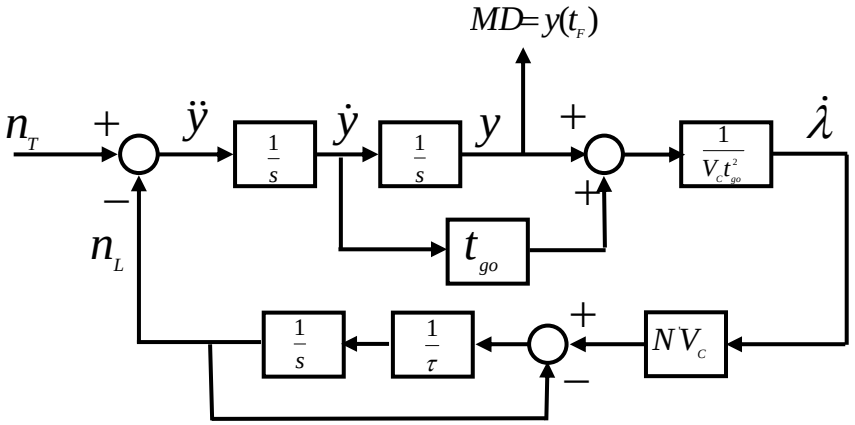

Figure 14: Linear Model B

In the literature, these two models (Model A and Model B) are often used interchangeably as the basis for a preliminary analysis of the performance of the generic guided missile homing loop [1-6]. The next section covers a comparison of the two models through the use of simulation and highlights input conditions under which the models yield different results. For these input conditions, caution should be exercised by the analyst when adopting these models, particularly when considering Model A.

4. Comparison of the Linearised Models

The two linear models have been implemented in Simulink in preparation for a comparative simulation study. The Simulink implementation of Model A and B are presented in Figures 15 and 16, respectively. For the present work, the simulations of the linear models are carried out under the same input conditions considered in Section 2.2 above. This allows a comparison of the simulation results generated by the linear models against those obtained by the non-linear model. To do this, the time of intercept displayed in the GUI after running the non-linear

model is recorded as the approximate flight time, t_F, for the engagement. This flight time is then used in the linear models. Additionally, the same numerical values for the parameters are used, as shown in the GUI in Figure 3.

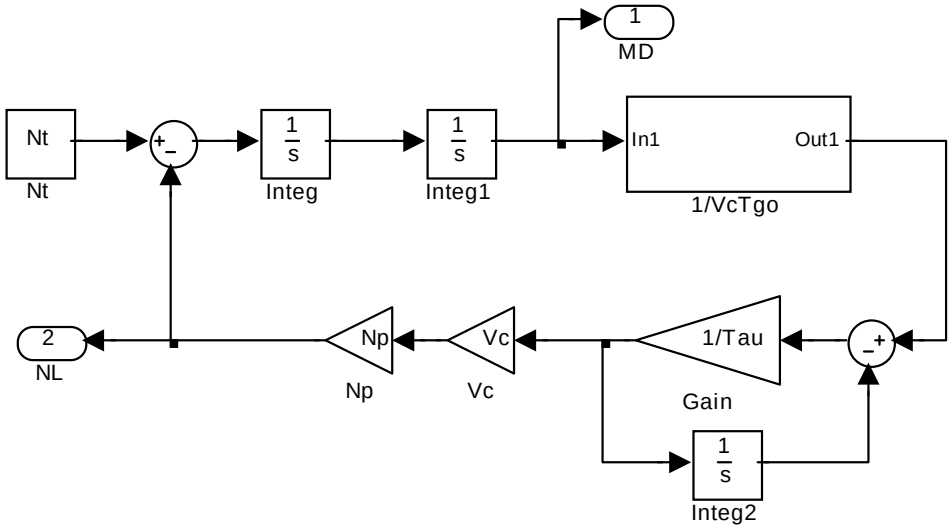

Figure 15: Simulink Implementation of Linear Model A

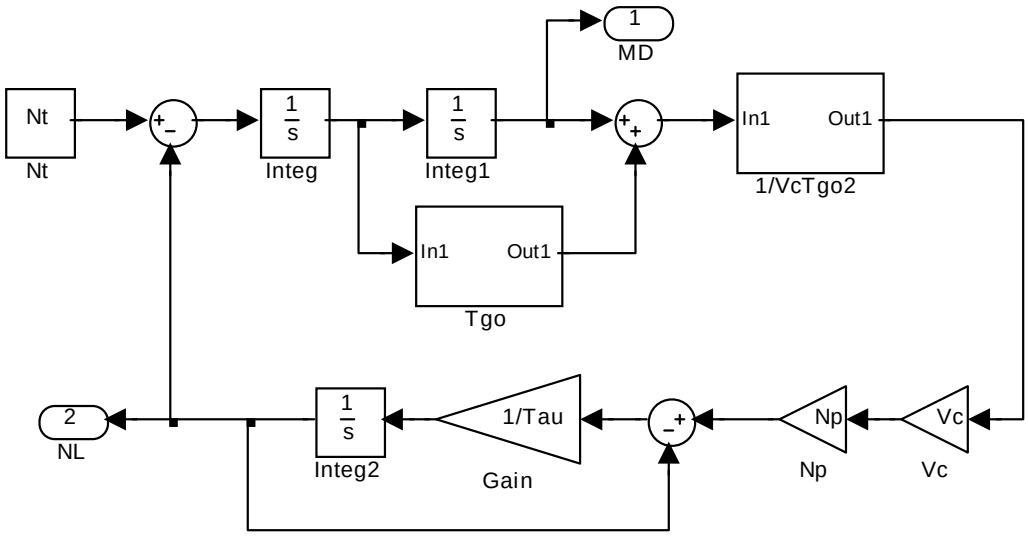

Figure 16: Simulink Implementation of Linear Model B

4.1.1 Step in target manoeuvre

A step in target acceleration of magnitude $3g$ is applied to both linear models and all other inputs are set to zero. The simulation results are presented in Figures 17 and 18 below. Figure 17 shows the time history of the relative displacement profile while Figure 18 shows the achieved missile acceleration profile. It is clear from the figures that both Model A and

Model B simulation results agree. Furthermore, the linear models provide a good approximation to the non-linear engagement model in this case.

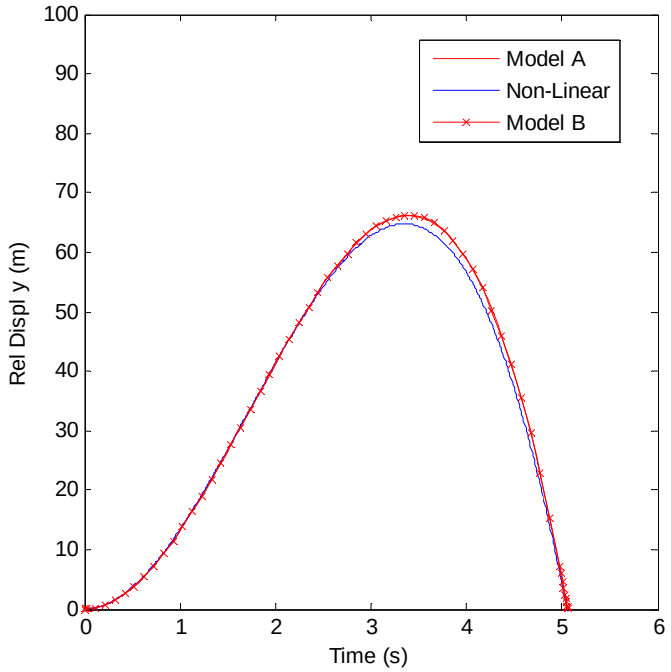

Figure 17: Comparison of relative displacement profile in the case of a 3g step in target manoeuvre

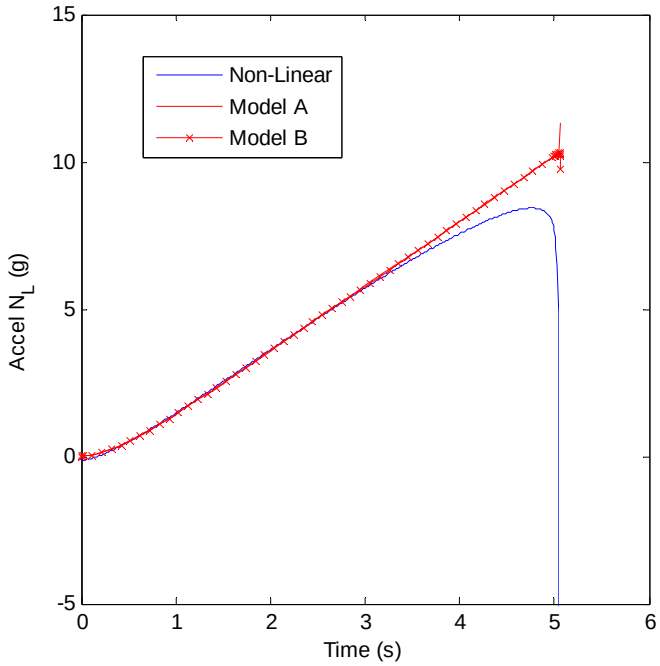

Figure 18: Comparison of missile acceleration profile in the case of a 3g step in target manoeuvre

4.1.2 Heading error

In this case, an error in initial heading angle of -20 degrees is considered with all other inputs set to zero. Again, the simulation results from the linear models are compared with those generated by the non-linear engagement model. The heading error is introduced in the linear models as an appropriate initial condition on the first integrator in the Simulink model of Figure 15 and 16, respectively. The results of the simulations are presented in Figure 19 and 20 below.

The figures indicate that both linear models agree in this case and that they represent a good approximation to the dynamics of the non-linear engagement model.

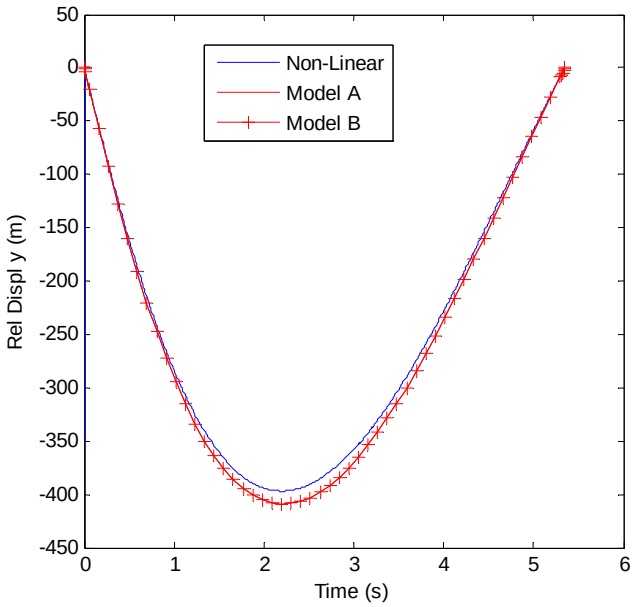

Figure 19: Comparison of relative displacement profile in the case of a heading error of -20 deg

4.1.3 Step in target position

Here, interest lies in the response of the missile to a sudden step in target position at a certain time to go prior to intercept. This scenario simulates the effect of target resolution by the on-board seeker in a multi-target scenario. For the linearised models, this condition translates into an appropriate initial condition placed on the second integrator (Integ1) in Figures 15 and 16.

Simulink simulations were carried out for both linear models and then compared to the corresponding non-linear results, as shown in Figures 20 and 21 below. These plots show that Model A results do not agree with Model B results. Furthermore, the plots demonstrate that Model B results are a good approximation to the simulation results generated by the non-linear model. However, the same cannot be said of Model A in this case.

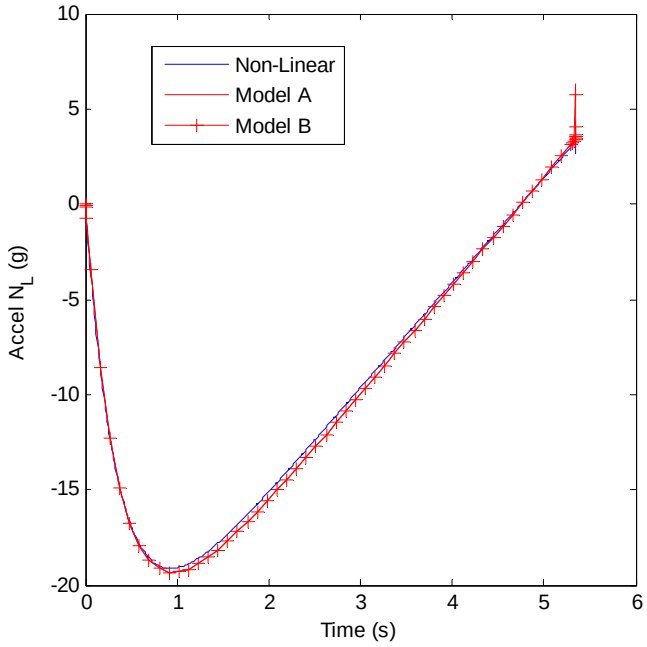

Figure 20: Comparison of missile acceleration profile in the case of a heading error of -20 deg

Consequently, the observations gleaned from the foregoing simulations suggest that Model B is a sufficiently accurate linear model when considering the missile target engagement problem. And this is so regardless of the three input conditions considered. However, caution needs to be exercised when using Model A for this purpose as it has been shown via simulation to produce erroneous results under one of the stipulated input conditions (see Figure 21 and 22).

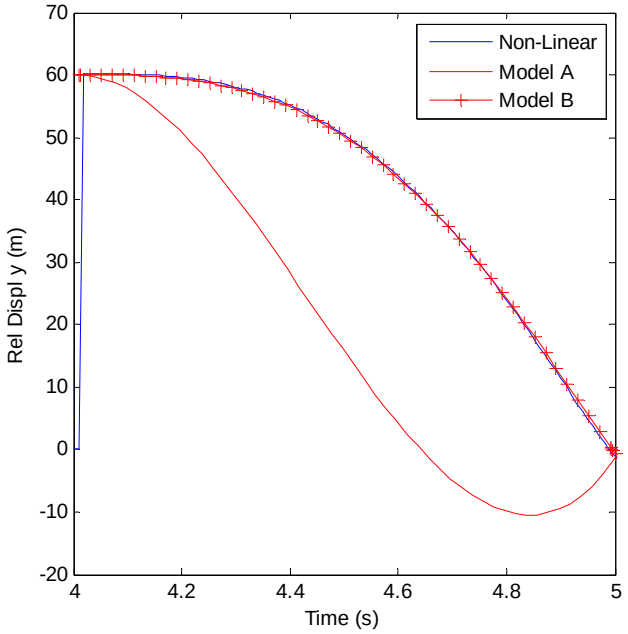

Figure 21: Comparison of relative displacement profile in the case of a jump in target position of 60 m

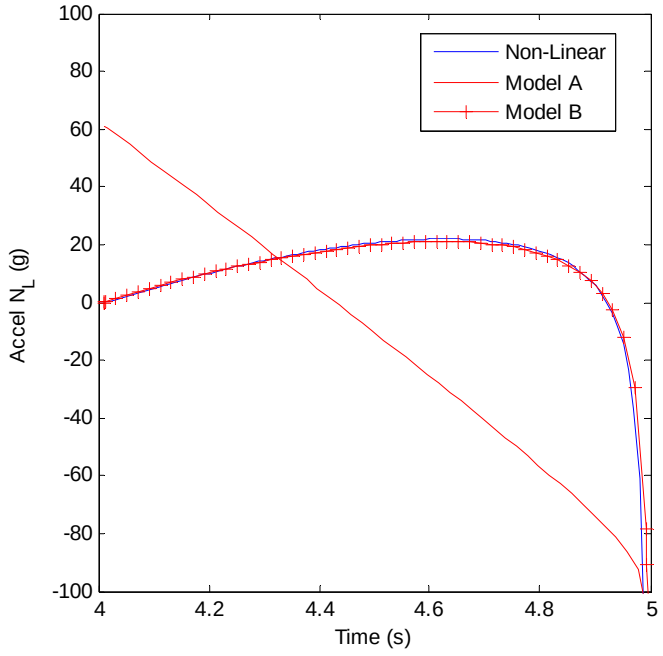

Figure 22: Comparison of missile acceleration profile in the case of a jump in target position of 60 m

5. Derivation of a Correction for Model A

In this section, an analysis is carried out to explore whether Model A can be brought into alignment with Model B when the input condition is a step in target displacement. Consider the block diagram of Model A given in Figure 13 and reproduced in Figure 23 for convenience. In Figure 23, the states of the system have been included in the block diagram, designated by x_i, as has the desired input condition y_{ic}.

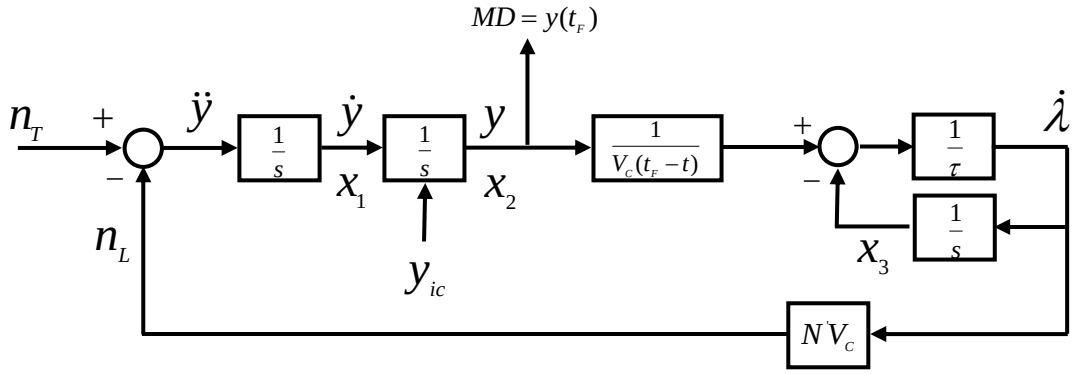

Figure 23: Linear Model A with system states displayed

By inspection of the diagram, the state space equations may be easily written down. They are,

$$\dot{x}_1 = n_T - N'V_C\dot{x}_3 \,, \tag{28}$$

$$\dot{x}_2 = x_1 \,, \tag{29}$$

$$\dot{x}_3 = \frac{1}{\tau}\left(\frac{x_2}{V_C t_{go}} - x_3\right). \tag{30}$$

In this case, the initial conditions are, $x_1(0) = 0$, $x_2(0) = y_{ic}$ and $x_3(0) = 0$. Thus, for time zero, equation (30) yields

$$\dot{x}_3(0) = \frac{1}{\tau}\frac{y_{ic}}{V_C t_F}. \tag{31}$$

Consequently, the initial value of the relative acceleration $\ddot{y}(0)$ will have the magnitude

$$\ddot{y}(0) = \dot{x}_1(0) = n_T - \frac{N' y_{ic}}{\pi t_F}. \tag{32}$$

This is physically impossible as it implies a jump in missile achieved acceleration whenever the initial condition on y is non-zero. To counteract this effect, a requirement is placed on the filter initial condition as follows,

$$x_3(0) = \frac{y_{ic}}{V_C t_F}. \tag{33}$$

When this correction, in the form of a non-zero initial condition on the filter, is applied to Model A, the simulation results generated by both linear models agree as shown in Figure 24 and 25 below.

Thus, in conclusion, any of the linear models, Model A or Model B, derived previously may be used for linear analysis of the missile target engagement problem provided that Model A is used in conjunction with the correction factor derived above. It is noteworthy to point out that in the case when y_{ic} is zero, no initial correction of the filter is necessary.

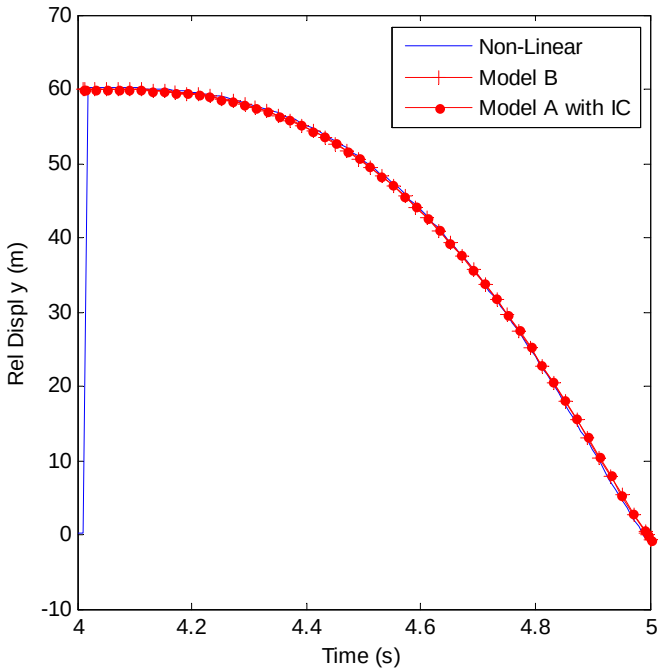

Figure 24: The relative displacement profile generated by the linear models now agree for the initial displacement case

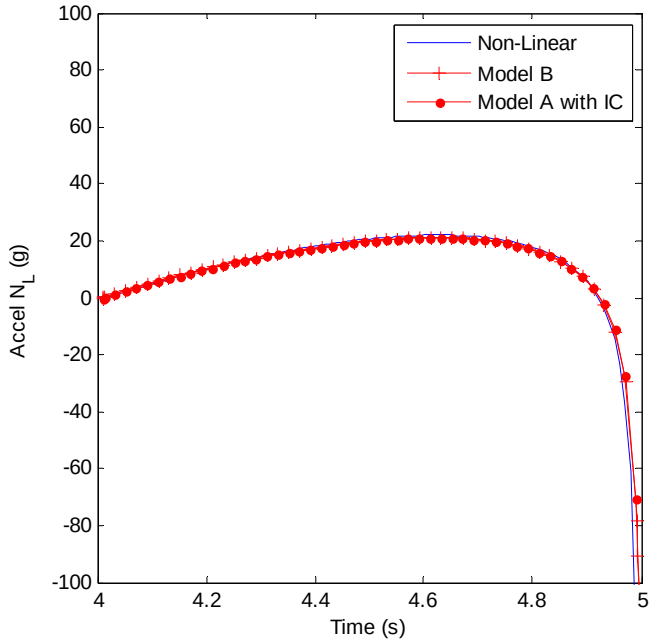

Figure 25: The missile acceleration profile generated by the linear models now agree for the initial displacement case

6. Analytical Formulas

The linearisation of the engagement model is important for two reasons. Firstly, with a linear model, powerful computerised techniques, such as the adjoint method, may be utilised to analyse the missile guidance system both statistically and deterministically in one computer simulation. Moreover, with this technique, error budgets are automatically generated so that key system drivers may be identified and a balanced system design can be achieved. Secondly, under special circumstances, the linear engagement model is mathematically amenable to analytical solutions. These solutions can assist, during the preliminary phases of a missile design, in gaining insights for system sizing. Furthermore, the form of the analytical solutions will provide clues on how key parameters may influence system performance.

In this section, closed-form solutions are derived for the three important cases that were considered above for the engagement simulations. The aim is to derive closed-form solutions associated with Model A and Model B independently and then to show that these solutions are mathematically equivalent provided that the filter initial condition is included in Model A. It has been shown in the literature [1] that closed form solutions for the linear engagement model may be obtained more easily using the adjoint method. Therefore, this is the method employed in the derivation process.

6.1 Closed-Form Solutions for Model A

The adjoint block diagram of Model A is presented in Figure 26. This model was constructed from the forward loop model given in Figure 13 using the usual rules of adjoint construction given in references [1, 3]. Note that x_{ic} in the diagram refers to the filter initial condition derived in the last section and is expressed, in this case, as

$$x_{ic} = \frac{y_{ic}}{V_C t_F}. \tag{34}$$

Also in the diagram, the initial condition for the heading angle error is defined as

$$HA = -V_M HE. \tag{35}$$

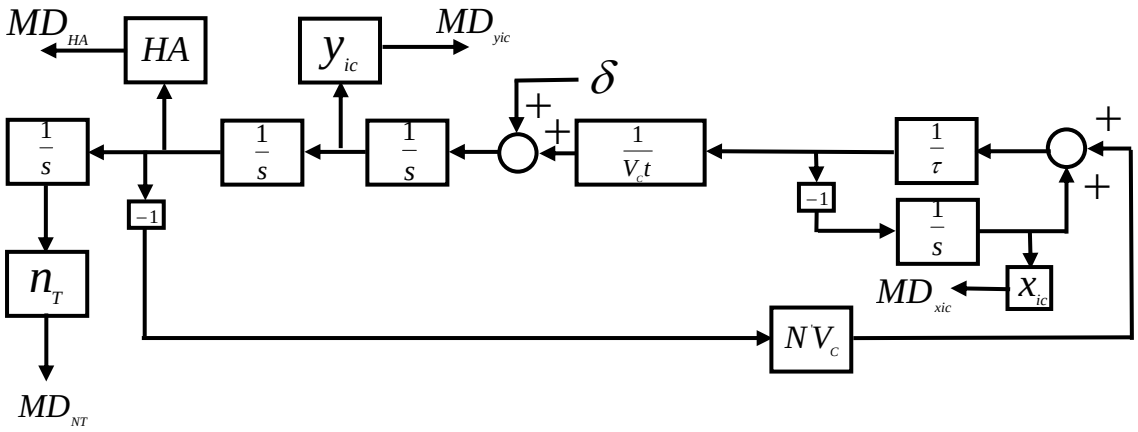

Figure 26: Adjoint Model A

In this form, the state equations associated with the adjoint block diagram (Figure 26) are mathematically challenging for analytical work. However, using block diagram algebra [1], the structure of this block diagram may be conveniently reduced to a form such as to allow easy mathematical treatment of the problem. The reduced form of the block diagram is presented in Figure 27 below. In the diagram, $h(t)$ is designated as an adjoint output signal while the weighting function $w(t)$, after frequency domain transformation, is defined as

$$W(s) = \frac{N'}{s(1+\tau s)}. \tag{36}$$

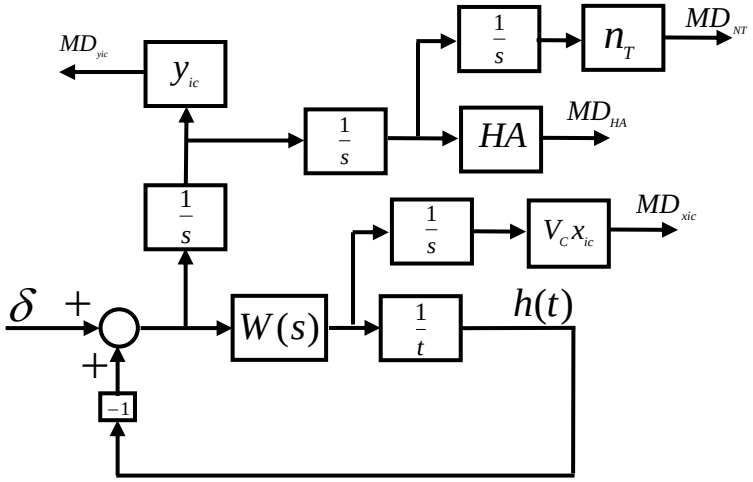

Figure 27: Reduced Form of Adjoint Model A

Using the convolution integral, the adjoint output is related to the input by

$$h(t) = \frac{1}{t}\int_0^t w(\eta)[\delta(t-\eta) - h(t-\eta)]d\eta \,. \tag{37}$$

After taking the Laplace Transform of the preceding equation, one obtains

$$-\frac{dH}{ds} = W(s)[1-H(s)] \,. \tag{38}$$

However, since

$$-\frac{dH}{ds} = \frac{d}{ds}[1-H(s)] \ , \tag{39}$$

the technique of separation of variables is invoked to arrive at

$$\int \frac{d(1-H)}{1-H} = \int W(s)ds \ . \tag{40}$$

The solution to equation (40) is given by

$$1-H(s) = C\exp(\int W(s)ds) \ , \tag{41}$$

where C is a constant of integration. This constant can be evaluated by first noting from Figure 27 that the miss distance due to a step in target displacement of magnitude y_{ic} is given by (using frequency domain notation)

$$L\{MD_{y_{ic}}\} = \frac{y_{ic}}{s}[1 - H(s)] \ . \tag{42}$$

In the above expression, the term $L\{\ \}$ refers to the Laplace transform of its argument. Let the magnitude of the step be unity. Then, in the time domain, the miss distance due to a unit step in target displacement at time zero will be unity. Thus, invoking the initial value theorem leads to

$$MD_{y_{ic}}(0) = 1 = \lim_{s \to \infty} s\left(\frac{1 - H(s)}{s}\right) \ . \tag{43}$$

Therefore, C is chosen to satisfy the following relation,

$$\lim_{s \to \infty} C \exp(\int W(s)ds) = 1 \ . \tag{44}$$

In this case, since $W(s)$ is given by equation (36), then it follows that $C = 1$, and equation (41) is reduced to

$$1 - H(s) = \exp(\int W(s)ds) \ . \tag{45}$$

Consequently,

$$\int W(s)ds = N' \int \frac{ds}{s(1 + \tau s)} \ , \tag{46}$$

$$= N' \int [\frac{1}{s} - \frac{1}{(s + 1/\tau)}]\, ds \ , \tag{47}$$

$$= N' \ln\left(\frac{s}{s + 1/\tau}\right) \ . \tag{48}$$

Now, after substitution of this expression into equation (45) above, one obtains the fundamental relationship

$$1 - H(s) = \left(\frac{s}{s + 1/\tau}\right)^{N'} \ . \tag{49}$$

Consequently, from inspection of the adjoint block diagram given in Figure 27 above, it is easy to write down expressions (in frequency domain notation) for each of the desired outputs as follows. The miss distance due to a step manoeuvre of magnitude n_T is given by

$$L\{\frac{MD_{NT}}{n_T}\} = \frac{1-H(s)}{s^3} = \frac{1}{s^3}\left(\frac{s}{s+1/\tau}\right)^{N'} \quad . \tag{50}$$

The miss distance due to an initial heading error is given by

$$L\{\frac{MD_{HE}}{HE}\} = -V_M \frac{[1-H(s)]}{s^2} = \frac{-V_M}{s^2}\left(\frac{s}{s+1/\tau}\right)^{N'} \quad . \tag{51}$$

For a step in target displacement, the miss distance formula is composed of two parts, namely, that due to y_{ic} and that due to x_{ic}. The part due to y_{ic} is

$$L\{\frac{MD_{yic}}{y_{ic}}\} = \frac{1-H(s)}{s} = \frac{1}{s}\left(\frac{s}{s+1/\tau}\right)^{N'} \quad , \tag{52}$$

while the part due to x_{ic} is, according to Figure 27,

$$L\{\frac{MD_{xic}}{V_C x_{ic}}\} = \frac{[1-H(s)]W(s)}{s} = \frac{N'}{\tau s^2}\left(\frac{s}{s+1/\tau}\right)^{N'} \frac{1}{s+1/\tau} \quad , \tag{53}$$

Therefore, for an effective navigation ratio of 3, the inverse Laplace Transform of the above expressions is taken, yielding the analytical expressions in equations (54) and (55). Note that the time variable appearing in the expressions is adjoint time which may be interpreted as total flight time t_F for the engagement problem.

$$\left.\frac{MD_{NT}}{n_T}\right|_{N'=3} = 0.5 t_F^2 e^{-t_F/\tau} \quad , \tag{54}$$

and

$$\left.\frac{MD_{HE}}{HE}\right|_{N'=3} = -V_M t_F e^{-t_F/\tau}\left(1-\frac{t_F}{2\tau}\right) \quad . \tag{55}$$

Furthermore, the miss distance due to a step in target displacement may be determined by the addition of the inverse Laplace Transform of equations (52) and (53). The closed form expression for this is

$$\left(\frac{MD_{yic}}{y_{ic}}\right)_{Tot}\Bigg|_{N'=3} = \left.\frac{MD_{yic}}{y_{ic}}\right|_{N'=3} + \left.\frac{MD_{xic}}{y_{ic}}\right|_{N'=3} \quad , \tag{56}$$

where

$$\left.\frac{MD_{yic}}{y_{ic}}\right|_{N'=3} = [1-2\frac{t_F}{\tau}+0.5\frac{t_F^2}{\tau^2}]e^{-t_F/\tau}\ , \tag{57}$$

and

$$\left.\frac{MD_{xic}}{y_{ic}}\right|_{N'=3} = [1.5\frac{t_F}{\tau}-0.5\frac{t_F^2}{\tau^2}]e^{-t_F/\tau}\ . \tag{58}$$

In deriving equation (58) above, use was made of equation (34). Consequently, adding the above expressions yields the miss distance due to a step in target displacement of magnitude y_{ic}, namely

$$\left.\left(\frac{MD_{yic}}{y_{ic}}\right)_{Tot}\right|_{N'=3} = [1-0.5\frac{t_F}{\tau}]e^{-t_F/\tau}\ . \tag{59}$$

6.1.1 Adjoint of Model A in Simulink

A Simulink model of the adjoint system of Model A (Figure 26) is shown in Figure 28. This model is used to generate simulation data for comparison with the closed form solutions given previously. The comparisons are displayed in the following figures.

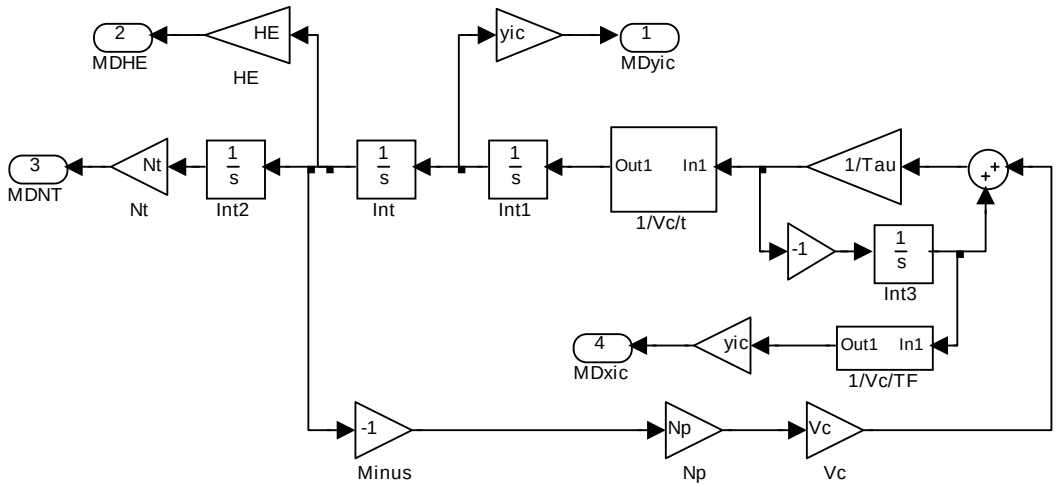

Figure 28: Adjoint Model A in Simulink

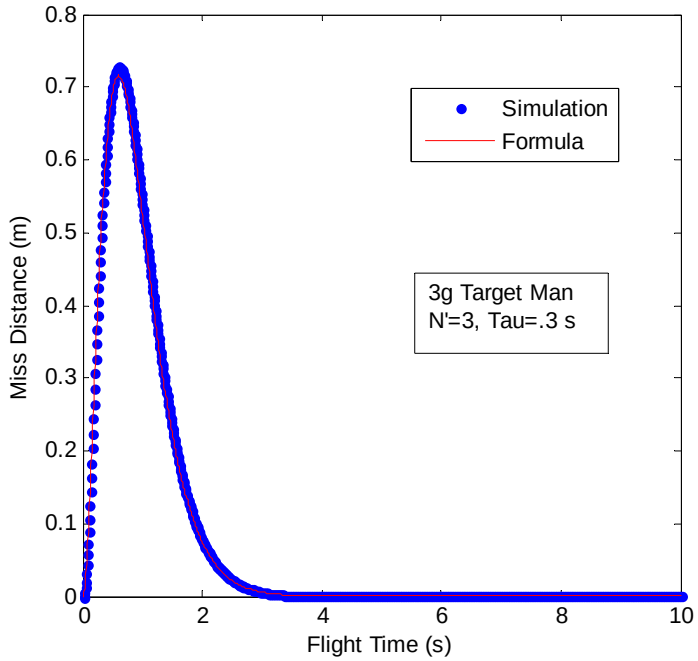

Figure 29: Adjoint Simulation and Formula agree for MD_{NT}

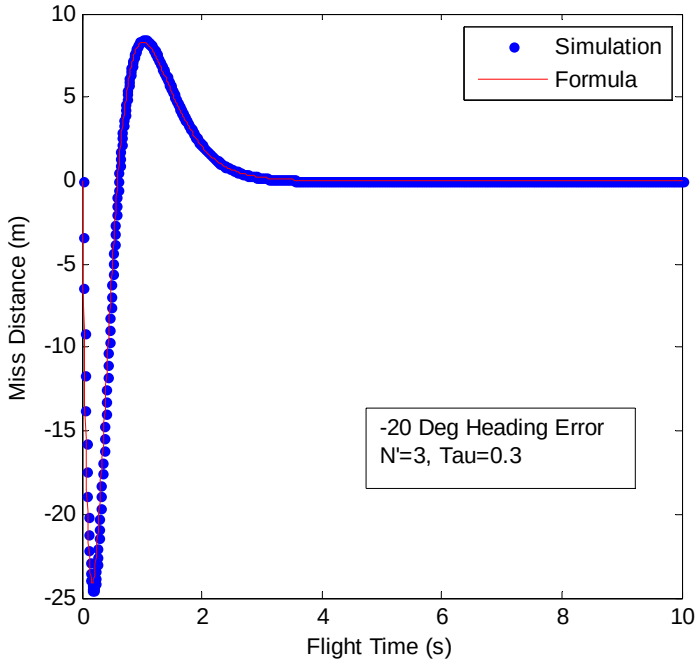

Figure 30: Adjoint Simulation and Formula agree for MD_{HE}

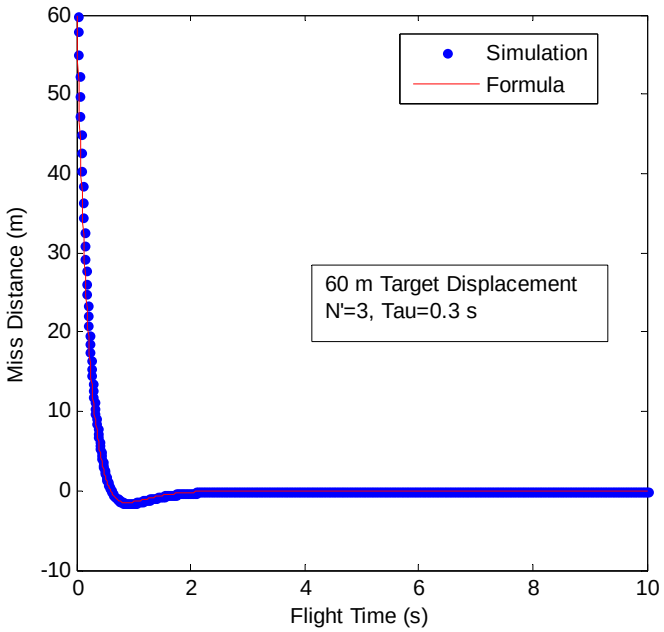

Figure 31: Adjoint Simulation and Formula agree for MDyic

The plots confirm that the closed form solutions and the Simulink simulation results based on the linear adjoint of Model A agree for the particular cases considered here. Thus, either approach may be used for preliminary system design. Recall that the closed form solutions are based on a single time constant guidance loop. However, for higher order systems, the equations become mathematically intractable. Thus, using the simulation model allows the analyst added flexibility for studying more complex homing loop systems with minimum extra effort due to the block diagram features of Simulink. This aspect shall be considered further in a later section of the report.

6.1.2 Comparison with non-linear results

Here, the non-linear engagement model, as presented in Section 1, is used in a multi-run mode to generate the miss distance profile as a function of flight time or time to go. This will enable a comparison of the non-linear simulation results with those obtained using either the linear adjoint model in Simulink or the closed form solutions derived earlier. For the non-linear model, the approximate miss distance calculation method, as employed by Zarchan [1], is utilised. Furthermore, in order to obtain the miss distance profile as a function of flight time using the non-linear simulation, a range to go parameter is defined and utilised in the process.

The miss distance generated using the non-linear model for a step in target manoeuvre of magnitude $3g$ is shown in Figure 32 for different flight times. Superimposed on this plot is the miss distance profile computed from the closed form solution for this scenario. It is clear from this plot that the closed form solution provides sufficiently accurate results for low values of flight time. As the flight time increases, the plot shows that the non-linear results tend to

diverge. According to linear theory, the miss distance tends to zero for flight times that are approximately greater than ten times the missile response time constant. This is clearly evident in the figure as the missile time constant is 0.3 in this case. Consequently, beyond a flight time of 3 seconds, linear theory is less accurate in this case.

In Figure 33, the non-linear simulation results are compared with those obtained using the closed form solution for the case of an error in initial missile heading angle. In this case, good agreement is obtained for most of the flight times considered. Large discrepancies occur when the total flight time is very small. This stems from the fact that under such conditions, the engagement scenario is significantly non-linear. As a final comparison with the non-linear simulation, the case of a step in target displacement is considered. In this case, the non-linear simulation results were obtained by looping over different values of homing time, or THOM in Figure 3. Again, the closed form solutions, based on the linear analysis, agree reasonably well with the non-linear simulation results generated by the Simulink model (see Figure 34).

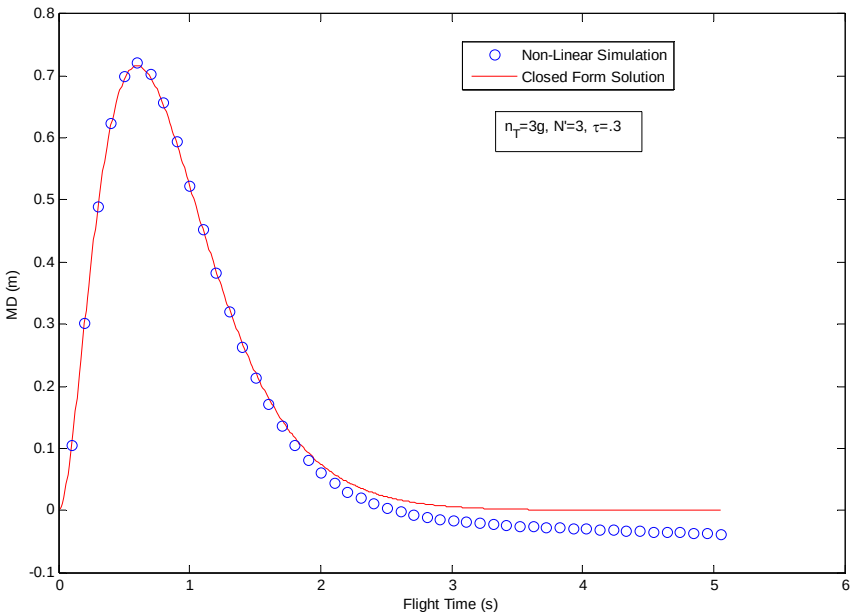

Figure 32: Formula agrees closely with non-linear simulation for MD_{NT}

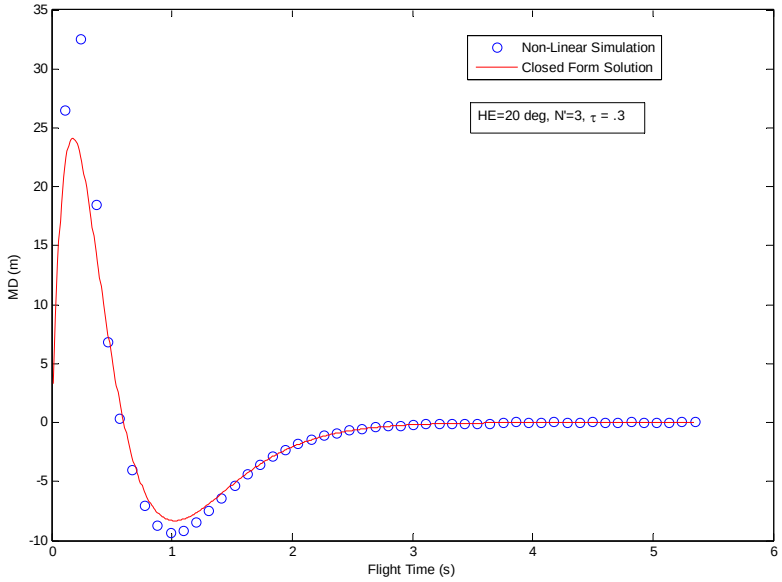

Figure 33: Formula agrees closely with non-linear simulation for MD_{HE}

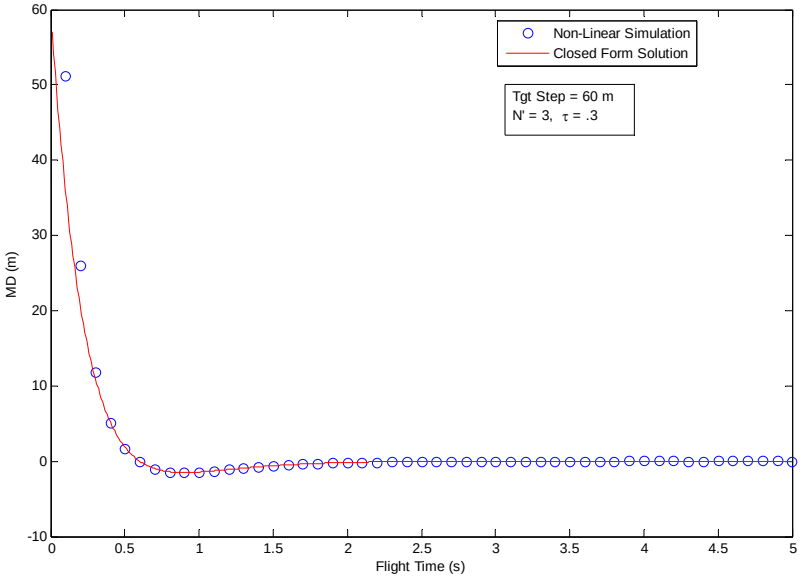

Figure 34: Formula agrees closely with non-linear simulation for MDyic

6.2 Closed-Form Solutions for Model B

In this section, linear Model B is investigated using analytical means. The forward loop block diagram of Model B is given in Figure 14. Applying the adjoint construction rules to this block diagram yields the adjoint block diagram of Model B as presented in Figure 35.

In Figure 35, the outputs of two of the integrators in the block diagram are designated as z_1 and z_2. These are clearly indicated in the figure. From inspection of the block diagram, the following expressions may be deduced, namely

$$\dot{z}_1 = z_2 + t\dot{z}_2, \quad z_2(0) = 1. \tag{60}$$

Consequently, after integrating this equation, one obtains the expression

$$z_1 = tz_2 + C_1 \quad , \tag{61}$$

where C_1 is a constant. The value of this constant can be determined by noting from Figure 35 that $z_1(t)$ is directly linked to the miss distance due to a heading angle error. Recall that the time variable in this case (adjoint model) is interpreted as flight time. Thus, for zero flight time, the following must be true, namely, $z_1(0) = C_1 = 0$. Consequently, equation (61) reduces to

$$z_1 = tz_2 \quad . \tag{62}$$

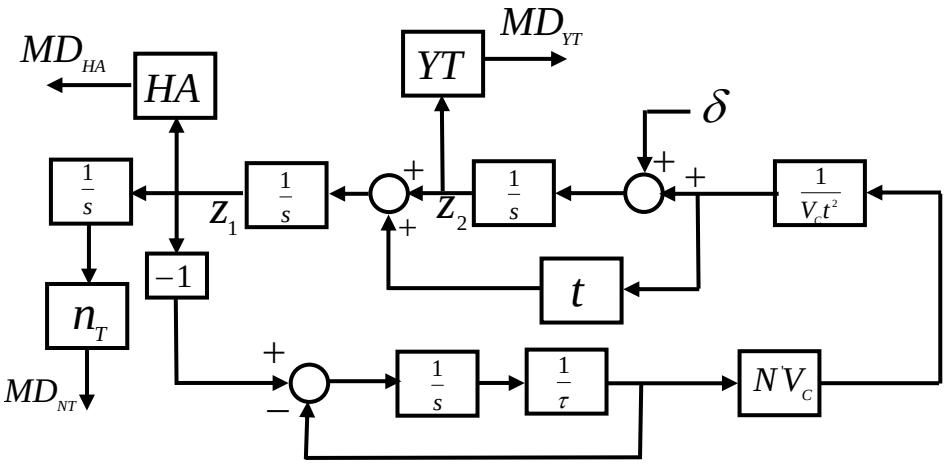

Figure 35: Adjoint Model B

Hence, making use of equation (62) above, and after introducing the expression for the weighting function defined earlier in equation (25), the block diagram displayed in Figure 35 may be judiciously manipulated into the block structure presented in Figure 36.

For ease of analysis, the block diagram displayed in Figure 36 is re-cast into the standard input-output form shown in Figure 37 below. Note that care must be exercised when doing this since the block diagram contains variables from different domains, that is, from the time domain (t) and the frequency domain (s). In the block diagram of Figure 37, two extra variables have been included as adjoint signals of interest, namely, $z_3(t)$ and $z_4(t)$.

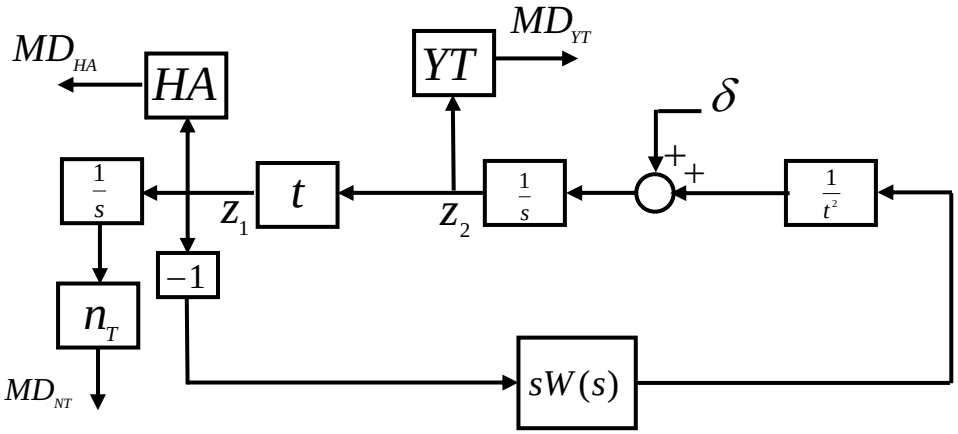

Figure 36: Equivalent block diagram of adjoint Model B

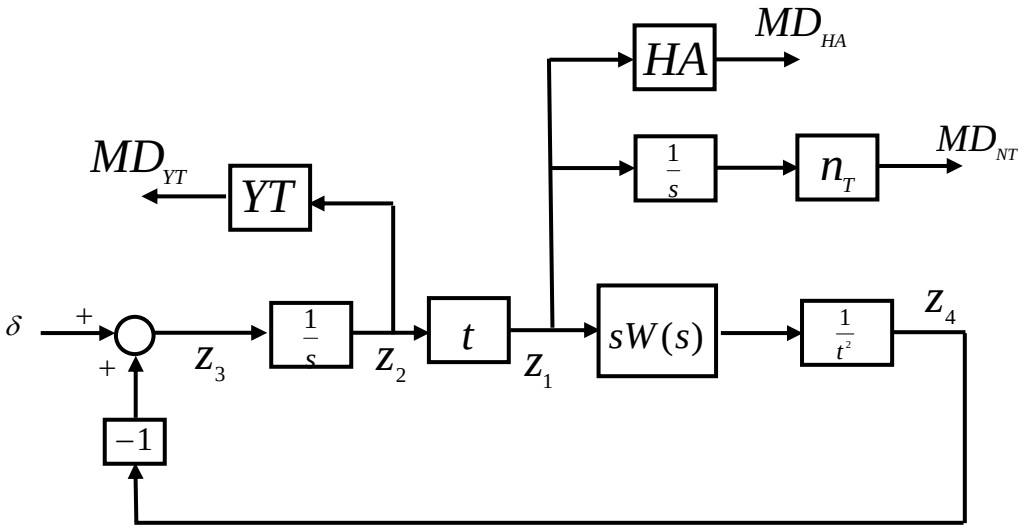

Figure 37: Equivalent block diagram in standard form

From Figure 37, the following time domain expressions may be deduced,

$$z_4(t) = \frac{1}{t^2}\int_0^t f(\eta) z_1(t-\eta)\, d\eta \quad , \tag{63}$$

$$z_2(t) = \int_0^t \frac{1}{\eta}[\delta(t-\eta) - z_4(t-\eta)]d\eta \quad , \tag{64}$$

where $f(t)$ is defined as

$$f(t) = L^{-1}\{sW(s)\} \quad . \tag{65}$$

Taking the Laplace Transform of equation (63) and (64) yields the following relationships,

$$\frac{d^2 Z_4(s)}{ds^2} = sW(s)Z_1(s) \quad , \tag{66}$$

$$Z_2(s) = \frac{1 - Z_4(s)}{s} = \frac{Z_3(s)}{s} \quad . \tag{67}$$

Furthermore, taking the Laplace Transform of equation (62), yields the relation

$$Z_1(s) = -\frac{dZ_2(s)}{ds} \quad . \tag{68}$$

After some algebra, the following differential equation for $Z_1(s)$ is derived,

$$\frac{dZ_1}{ds} + \left(\frac{2}{s} - W(s)\right)Z_1 = 0 \quad . \tag{69}$$

This differential equation may be readily solved using separation of variables to yield

$$Z_1(s) = \frac{C_2}{s^2} e^{\int W(s)ds} \quad , \tag{70}$$

where C_2 is a constant. The value of the constant may be determined as follows. From the block diagram in Figure 37, the expression for the miss distance due to target displacement may be derived. This has the form

$$MD_{YT} = YT * z_2(t) \quad . \tag{71}$$

Therefore, for a unit step in target displacement at zero flight time, the following condition must be true, namely,

$$z_2(0) = 1 \quad . \tag{72}$$

Note the consistency with equation (60) above, where the same condition arose as a result of the impulsive input.

After substituting the expression for $W(s)$, as defined in equation (25), into equation (70) above, and after some algebra, the following expression is obtained,

$$Z_1(s) = \frac{C_2}{s^2}\left[\frac{s}{s+1/\tau}\right]^{N} \quad . \tag{73}$$

From equation (62)

$$z_2(t) = \frac{z_1(t)}{t} \quad . \tag{74}$$

Thus at zero flight time, the following expression is valid,

$$z_2(0) = \lim_{t \to 0} \frac{z_1(t)}{t} \quad . \tag{75}$$

Using L'Hopital's rule and making use of equation (72) yields the expression,

$$1 = \lim_{t \to 0} \frac{dz_1}{dt} \quad . \tag{76}$$

Now, the Laplace Transform of dz_1/dt is given by

$$L\left\{\frac{dz_1}{dt}\right\} = sZ_1(s) - z_1(0) \quad . \tag{77}$$

However, as was shown earlier, $z_1(0) = 0$. Hence, the above expression reduces to

$$L\left\{\frac{dz_1}{dt}\right\} = sZ_1(s) \quad . \tag{78}$$

Consequently, returning to equation (76) and invoking the initial value theorem leads to the following expression

$$1 = \lim_{s \to \infty} s^2 Z_1(s) \quad . \tag{79}$$

Hence, after substituting equation (70) into equation (79), and making use of equation (25), the above expression reduces to

$$1 = \lim_{s \to \infty} C_2 \left[\frac{s}{s + 1/\tau} \right]^{N'} \quad . \tag{80}$$

This implies that $C_2 = 1$. Consequently, the expression for $Z_1(s)$ is

$$Z_1(s) = \frac{1}{s^2} \left[\frac{s}{s + 1/\tau} \right]^{N'} \quad . \tag{81}$$

This expression may now be used to deduce the Laplace Transform of the miss distance outputs of interest highlighted in Figure 37 above, namely, the miss distance due to target manoeuvre,

$$MD_{NT}(s) = \frac{n_T}{s^3} \left[\frac{s}{s + 1/\tau} \right]^{N'} \quad , \tag{82}$$

and the miss distance due to an initial heading error,

$$MD_{HA}(s) = \frac{-V_M HE}{s^2} \left[\frac{s}{s + 1/\tau} \right]^{N'} \quad . \tag{83}$$

Finally, the miss distance due to target displacement is found by making use of equation (74). After time domain conversion, this may be expressed as

$$MD_{YT}(t_F) = YT * z_1(t_F) / t_F \quad , \tag{84}$$

where t_F denotes flight time.

6.2.1 Closed Form Solutions for N'=3

Here closed form solutions are derived for a particular value of the navigation ratio, namely, $N' = 3$. Substitution of this value into the above expressions, and after taking the inverse Laplace Transform, yields the following closed form solutions,

$$\left. \frac{MD_{NT}}{n_T} \right|_{N'=3} = 0.5 t_F^2 e^{-t_F/\tau} \quad , \tag{85}$$

$$\left. \frac{MD_{HA}}{HE} \right|_{N'=3} = -V_M t_F e^{-t_F/\tau} \left(1 - \frac{t_F}{2\tau}\right) \quad , \tag{86}$$

$$\left. \frac{MD_{YT}}{YT} \right|_{N'=3} = e^{-t_F/\tau} \left(1 - \frac{t_F}{2\tau}\right) \quad . \tag{87}$$

These agree exactly with the corresponding formulas derived earlier and based on Model A. Closed form solutions may also be derived for other values of N′ provided they are integers. In fact, several of these closed form solutions have been derived and are reproduced in Appendix B. From the closed form solutions given above (and in Appendix B), it is clear that the miss distance due to a step in target displacement is related to the miss distance due to a heading error. This relationship is investigated further in Appendix C.

However, for non-integer values of N′, the mathematics is complex. In this case, the best approach for a solution would be to use simulation. A Simulink representation of Model B is displayed in Figure 38 below. As the simulation results agree exactly with those previously produced using Model A (see Figures 29-31), only those results generated using Model B will be presented here.

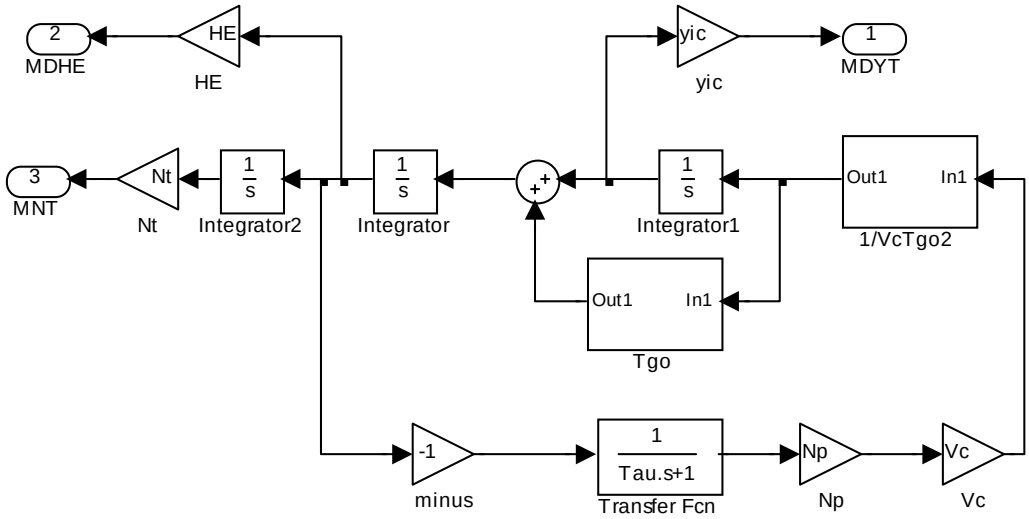

Figure 38: Adjoint Model B in Simulink

The miss distance due to a target manoeuvre of magnitude 3*g* (that is, output 3 in Figure 38) is presented in Figure 39 for various values of the proportional navigation ratio. From the same simulation, it is possible to extract similar information relating to the miss distance due to a heading error (output 2 in the figure) and the miss distance due to a step in target position (output 1 in Figure 38). These are presented in Figures 40 and 41 below. It is clear from these figures that the miss distance is generally smaller as the navigation ratio increases.

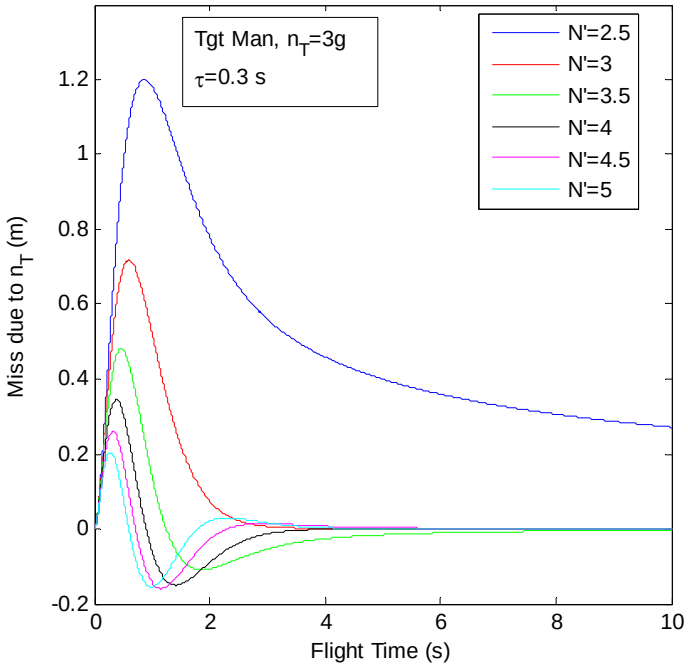

Figure 39: Miss due to Target Manoeuvre for Various N′

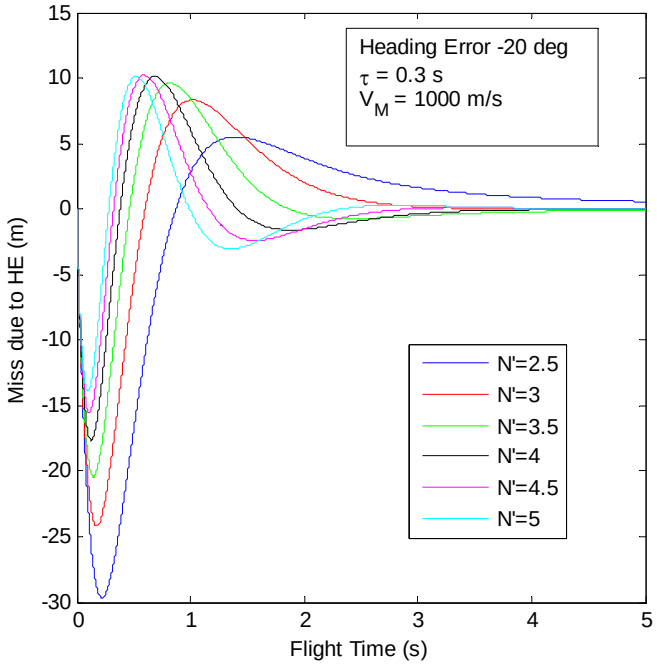

Figure 40: Miss due to Heading Error for Various N′

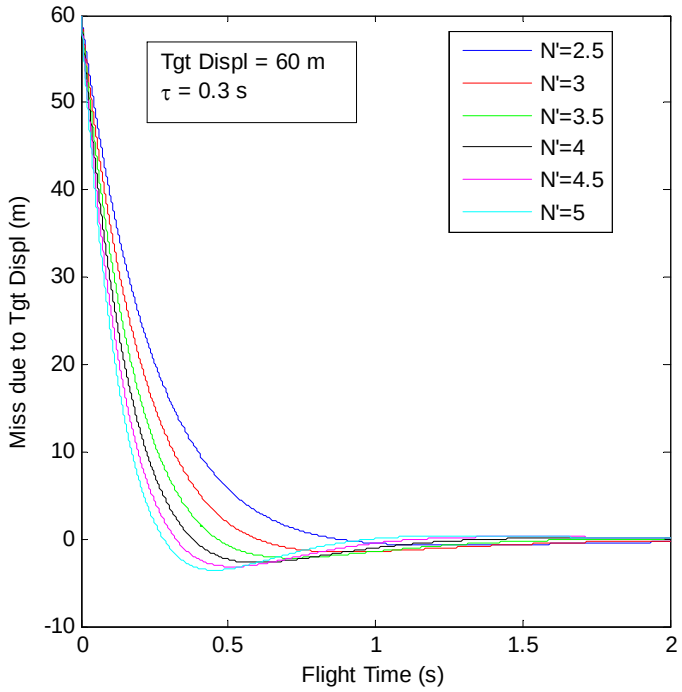

Figure 41: Miss due to Target Displacement for Various N'

7. Higher Order Guidance System Dynamics

It has been shown that when the guidance system dynamics may be characterised by a single time constant, then it is possible to derive closed form solutions for the miss distance. However, it is known from reference [1] that the single time constant representation of the guidance system seriously underestimates the miss distance. For a more realistic representation, reference [1] recommends the use of a fifth order transfer function representation. In this case, no closed form solution is possible. Thus the only option is to use numerical simulation.

In this section, the fifth order binomial model, as recommended by Zarchan [1], has been adopted. The model may be expressed in the form,

$$\frac{n_L}{\lambda} = \frac{N' V_C s}{(1+s\tau/5)^5} \quad , \tag{88}$$

Using the above model, it is shown that both linear models, namely, Model A and Model B, still produce equivalent simulation results provided that the correction term is applied to Model A as previously proposed for the single time constant case.

Firstly, Model A (see Figure 23) is modified to reflect the implementation of the fifth order guidance system representation expressed in equation (88) above. After a block diagram restructure, this new model is designated as Model A5 and is shown in Figure 42 below. Note that, as proposed earlier in the single time constant case, an initial condition x_{ic} on the first integrator downstream of the entry point has been included in the model to reflect the case of a step in target displacement y_{ic}. As previously, the value of this initial condition is given by the expression,

$$x_{ic} = \frac{y_{ic}}{V_C t_F}. \tag{89}$$

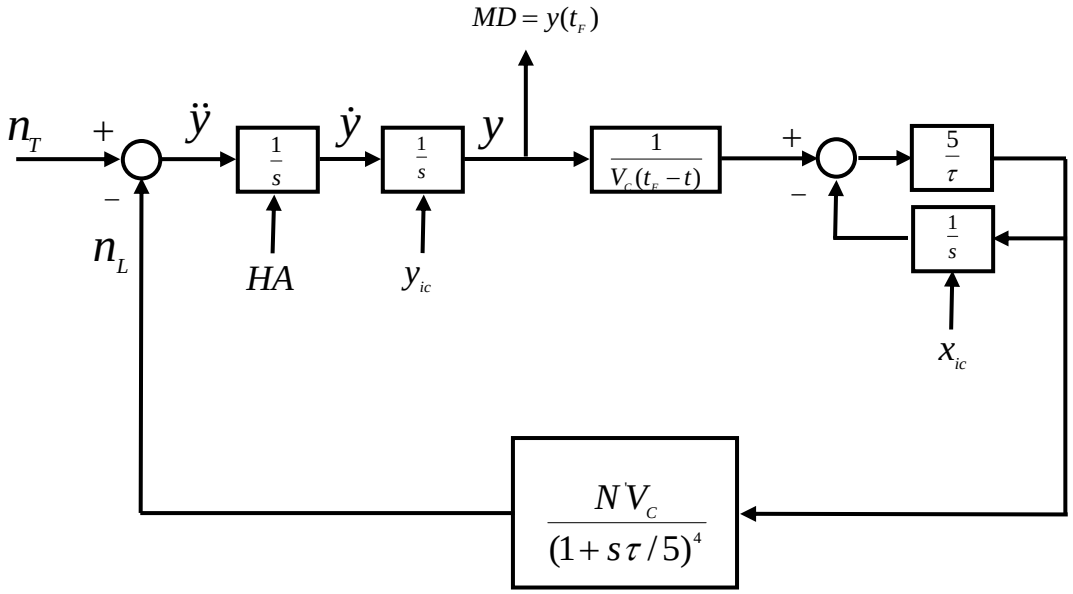

Figure 42: Block Diagram of Model A5

Now, following the adjoint construction rules given in [1, 3], it is an easy task to construct the adjoint of Model A5. This is shown in Figure 43.

In a similar fashion, the alternative adjoint model based on Model B is constructed. For the fifth order system, Model B is designated as Model B5. This is shown in Figure 44 and the corresponding adjoint model is shown in Figure 45.

Both models were then programmed in Simulink for subsequent adjoint simulation. The results are presented in Figure 46 through to Figure 48 inclusively. It is clear that both models yield the same results in this case and hence any of the models may be used interchangeably for the guidance loop analysis provided that the proposed correction strategy derived here is adopted when using Model A.

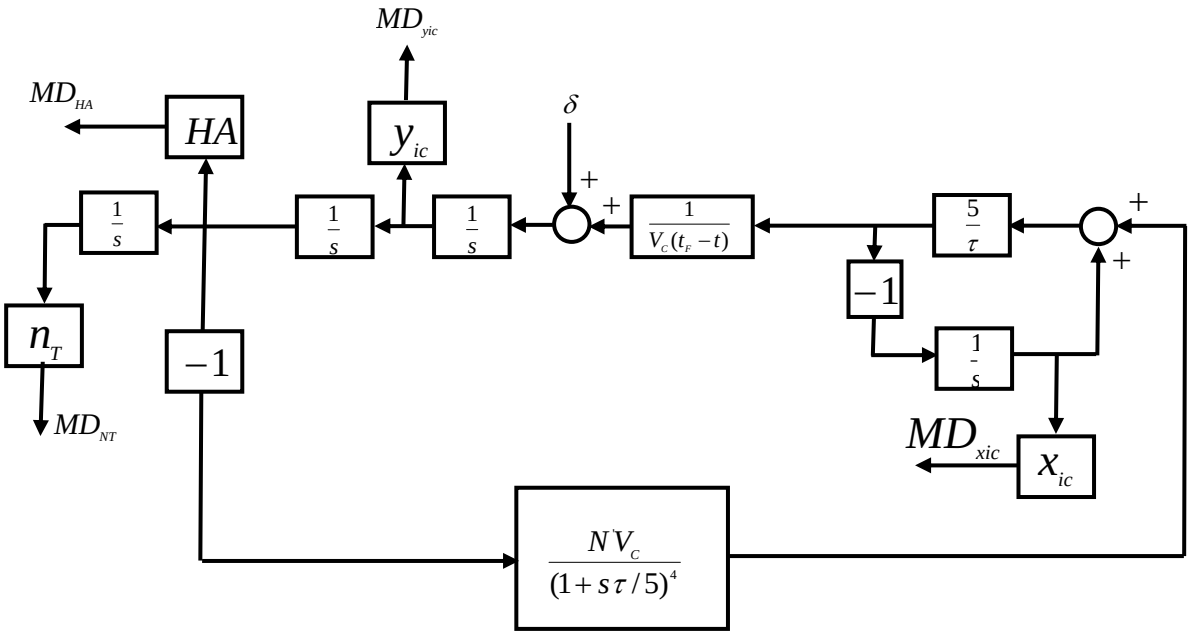

Figure 43: Adjoint Block Diagram of Model A5

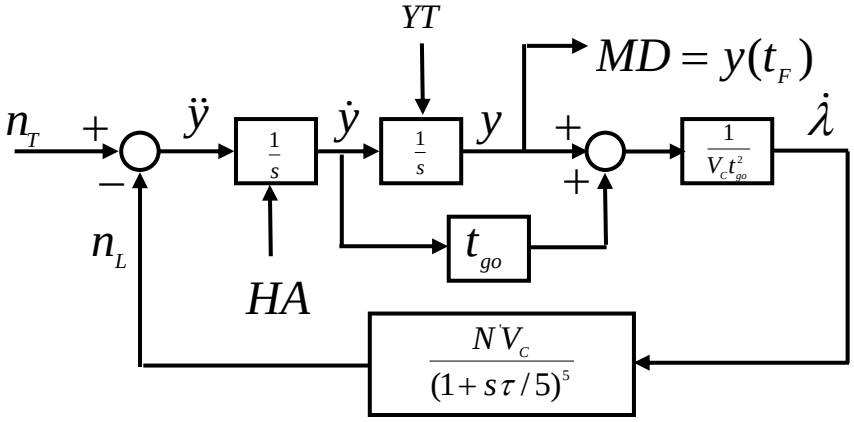

Figure 44: Block Diagram of Model B5

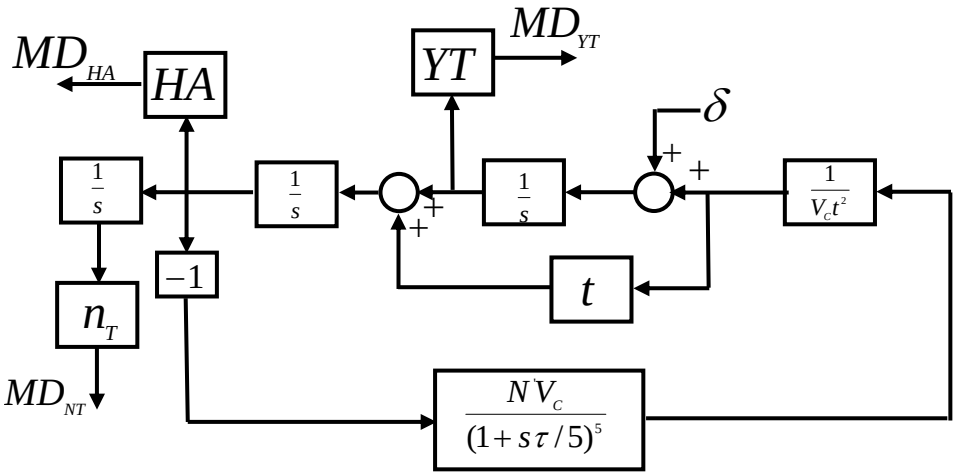

Figure 45: Adjoint Block Diagram of Model B5

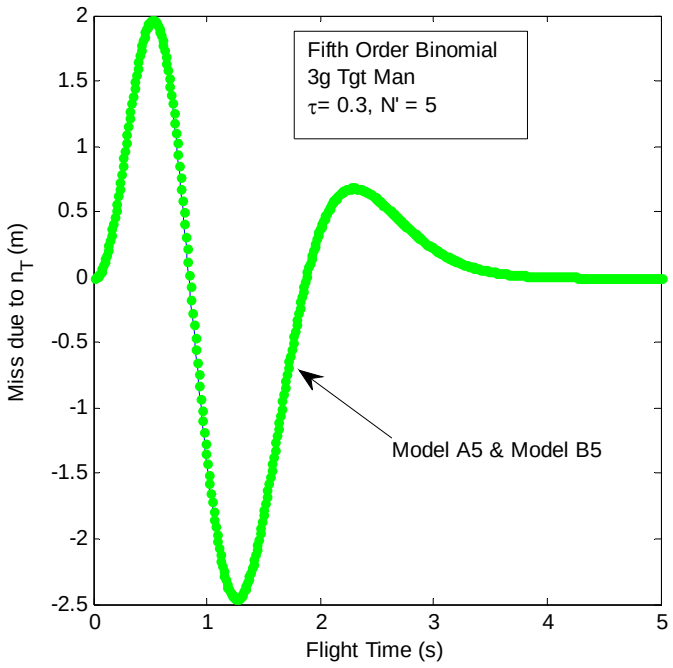

Figure 46: Miss Distance due to Target Manoeuvre for 5th Order System

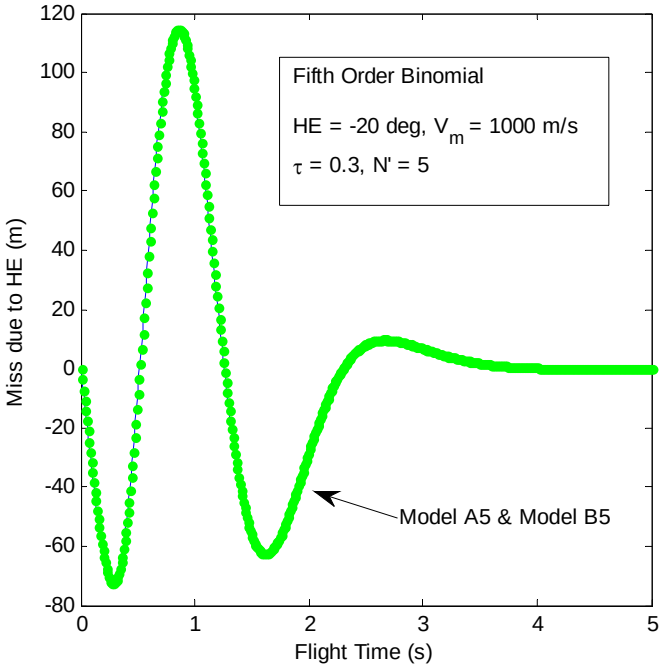

Figure 47: Miss Distance due to Heading Error for 5th Order System

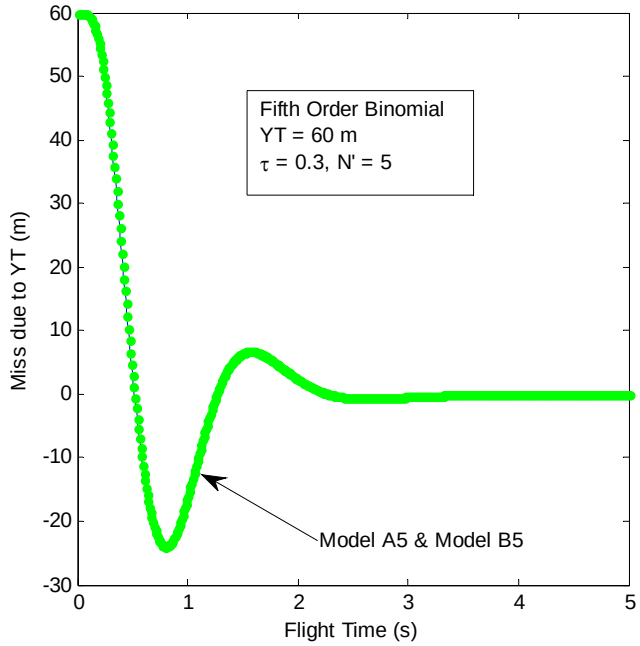

Figure 48: Miss Distance due to Target Displacement for 5th Order System

8. Conclusions

In this report, attention is focussed on the models and tools often adopted for the linear analysis of missile-target engagements in two dimensions. Following a review of the non-linear dynamic equations describing the problem, two linear models were developed for the linear analysis. These models are often used interchangeably in the literature for missile guidance loop analysis. However, it is shown here that under certain initial conditions of the state variables, the two models yield significantly different results. Hence, caution needs to be exercised by the analyst when adopting these models for missile homing loop analysis.

Following closer analysis, a correction factor was derived which may be used to render the two models equivalent. This correction factor was then used as the basis for deriving closed form solutions to the problem in the case when the guidance system may be approximately represented by a single time constant system. After carrying out the mathematics, it was demonstrated that both models yield the same closed form solution for the particular inputs considered.

The models were then implemented in Simulink and it was shown how they could be used for assessment of other problems in which the closed form solutions are not available. In addition to insights gained on system performance, another benefit of having derived the closed form solutions to this problem was the observation that two of the analytical relationships were indeed connected. Consequently, it was shown how this fact could be utilised for the generation of performance data associated with the study of multiple targets using the system response to a heading error input.

Finally, the power and flexibility of Simulink was utilised to demonstrate how easily these linearised engagement models and their adjoints could be extended to accommodate higher order and more complex dynamic system representations of the guidance loop.

9. References

1. Zarchan, P., "Tactical and Strategic Missile Guidance," 5th Ed. Progress in Astronautics and Aeronautics, Vol. 124, AIAA Inc. Washington DC, 2007.

2. Shneydor, N.A., "Missile Guidance and Pursuit, Kinematics, Dynamics and Control," Horwood Publishing Ltd, Chichester, UK, 1998.

3. Bucco, D., "Aerospace Applications of Adjoint Theory," Monograph, DSTO Fellowship Program, Australia, Jan 2010.

4. Gutman, S., "Applied Min-Max Approach to Missile Guidance and Control," Progress in Astronautics and Aeronautics, Vol. 209, AIAA Inc. Washington DC, 2005.

5. Weiss, M., "Adjoint Method for Missile Performance Analysis on State-Space Models," Journal of Guidance, Control and Dynamics, Vol. 28, No. 2, pp. 236-248, 2005.

6. Taylor, J.H., Price, C.F., Siegel, J. & Gelb, A., "Covariance Analysis of Nonlinear Stochastic Systems via Statistical Linearization," ASME, Nonlinear System and Synthesis, Vol. 2, Techniques and Applications, Feb 1981.

Appendix A: Non-linear Engagement Model in MATLAB/Simulink

A.1. Details of the Simulink Model

A.1.1 The Simulink Subsystem Models

The missile dynamics equations and the target dynamic equations are implemented in Simulink as subsystems, as shown in the figures below.

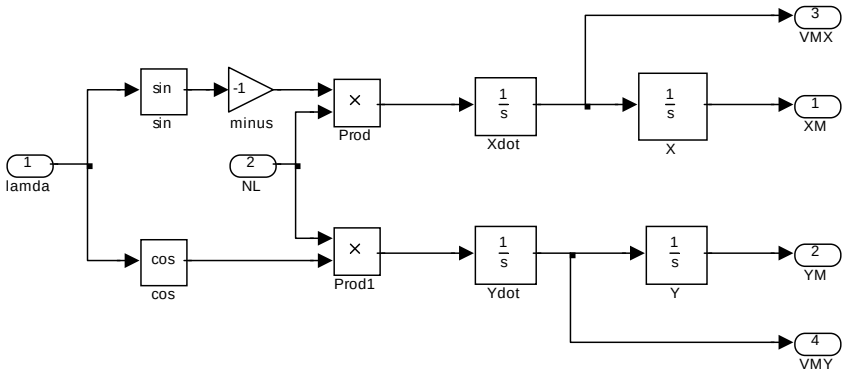

Figure A1. Missile Dynamics Subsystem

The Missile Dynamics Subsystem (Figure A1) contains all of the blocks required to simulate the missile dynamics as represented by the non-linear equations given in the text.

In a similar fashion, the Target Dynamics Subsystem (Figure A2) contains all of the blocks required to simulate the target dynamics in accordance with the target equations given in the text. In order to accommodate a sudden change in target position, a switch block has been included in the Simulink model. The switch, in this case, is used to simulate the different values of the target position to be represented in the simulation at the moment of seeker resolution in a multiple target scenario. It was necessary to insert a unit delay in the loop in order to avoid an inherent algebraic loop condition causing the simulation to fail.

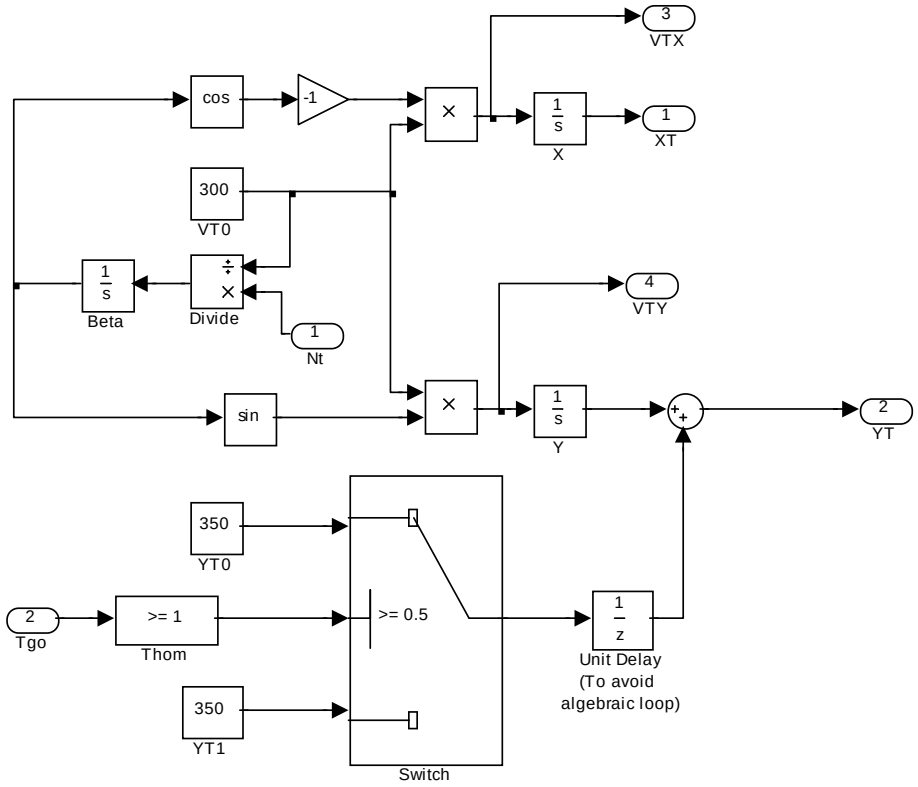

Figure A2. Target Dynamics

The implementation of the relative dynamics is shown in Figure A3.

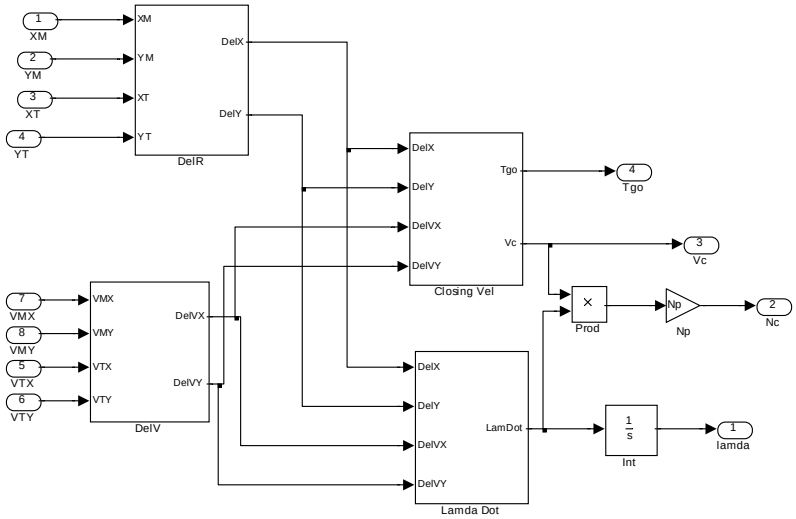

Figure A3. Relative Dynamics Subsystem

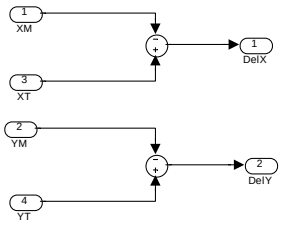

Figure A4. DelR Subsystem

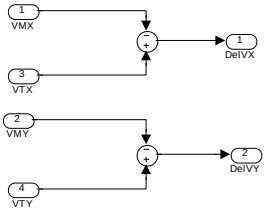

Figure A5. DelV Subsystem

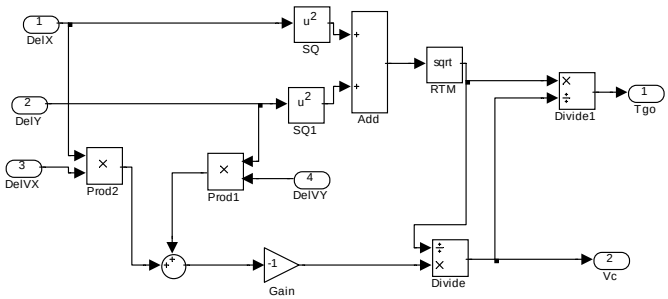

Figure A6. Closing Vel Subsystem

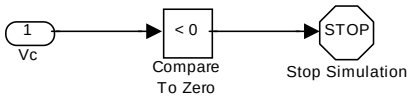

Figure A7. Stop Condition

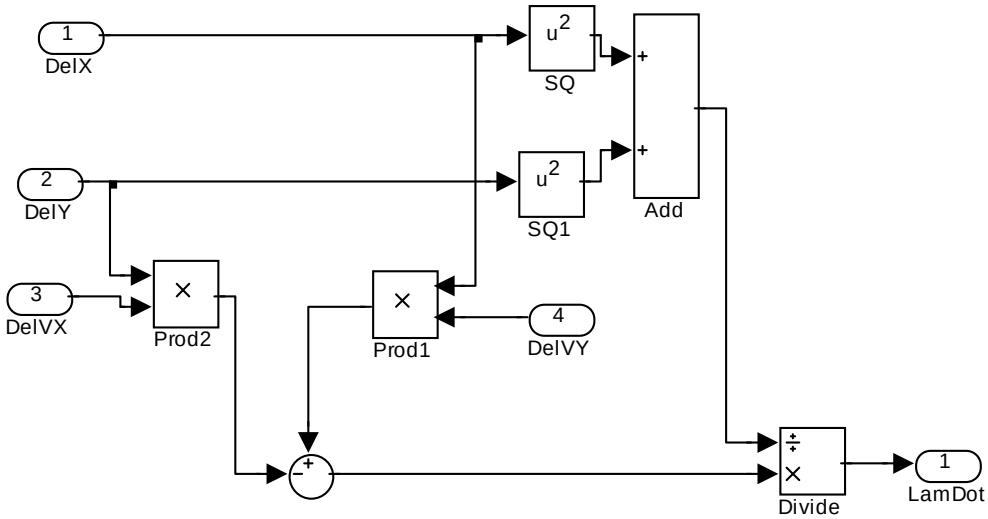

Figure A8. Lamda Dot Subsystem

Note that the Relative Dynamics subsystem block shown in Figure A3 is composed of the subsystems given in Figures A4, A5, A6 and A8. The simulation stopping condition model is shown in Figure A7.

A.1.2 The Associated MATLAB Code

The missile-target engagement model represented in Simulink is controlled by a Graphical User Interface underpinned by MATLAB code. The complete MATLAB code is listed over the following pages.

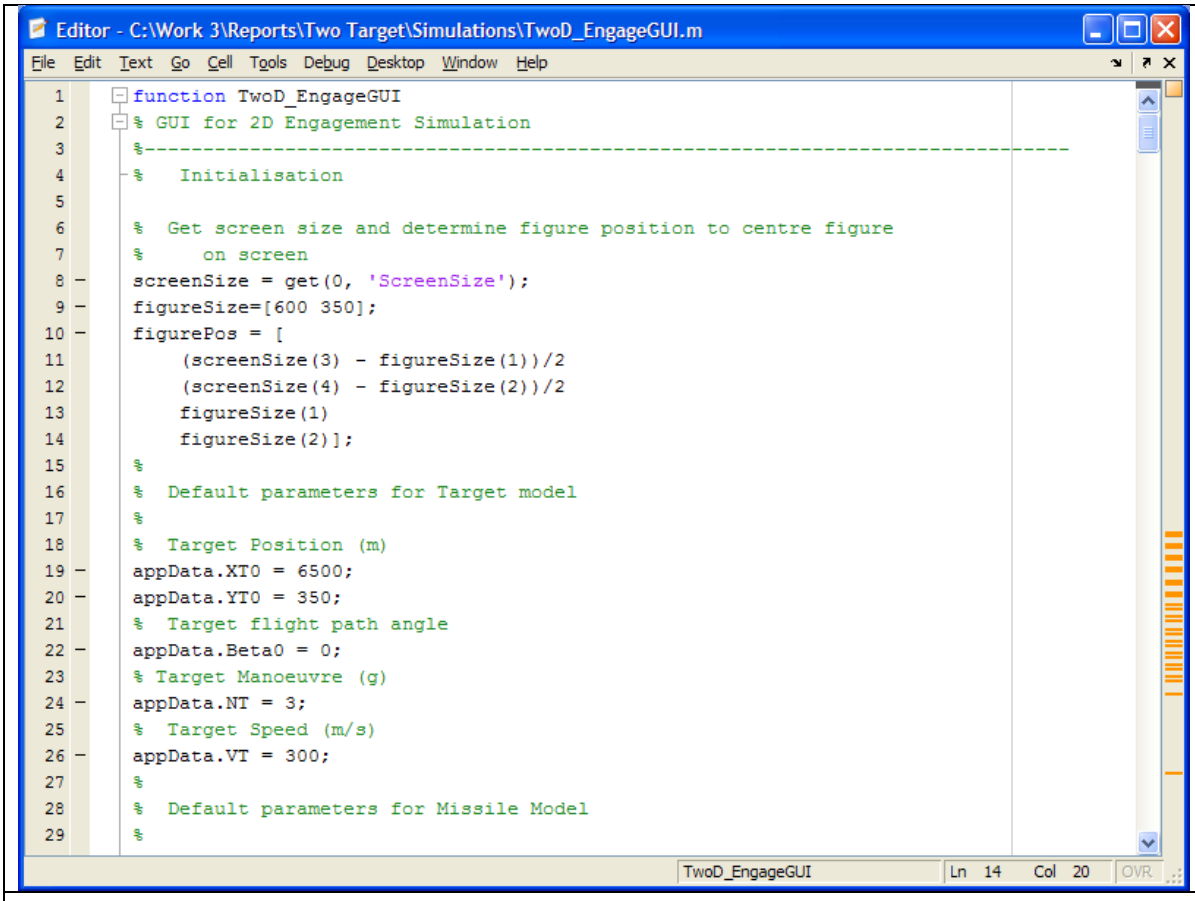

Figure A9. MATLAB Code

Editor - C:\Work 3\Reports\Two Target\Simulations\TwoD_EngageGUI.m

File Edit Text Go Cell Tools Debug Desktop Window Help

```
30    %  Missile Position (m)
31 -  appData.XM0 = 0;
32 -  appData.YM0 = 350;
33    %  Missile Speed (m/s)
34 -  appData.VM = 1000;
35    %  Missile Time Constant
36 -  appData.Tau = .3;
37    %  Effective Navigation Ratio
38 -  appData.Np = 3;
39    %  Heading Error (degrees)
40 -  appData.HE = 0;
41    %  Time to go when target resolution occurs
42 -  appData.Thom = 1;
43    %  Target Displacement when resolution occurs
44 -  appData.Displace = 0;
45    %
46    %   Initial Miss Value
47 -  appData.Tmiss = 0;
48 -  appData.Miss = 0;
49    % --- MAIN FIGURE -------------------------------------
50 -  GUIfig = figure(    'Tag', 'GUIfig', ...
51        'Units', 'pixels', ...
52        'Position', figurePos, ...
53        'Name', '2D Engagement', ...
54        'MenuBar', 'none', ...
55        'Resize','off',...
56        'NumberTitle', 'off', ...
57        'Color', get(0,'DefaultUicontrolBackgroundColor'));
58    % --- SUB PANEL - Target  -----------------------------------
```

TwoD_EngageGUI Ln 34 Col 19 OVR

Figure A10. MATLAB Code (continued)

Editor - C:\Work 3\Reports\Two Target\Simulations\TwoD_EngageGUI.m

File Edit Text Go Cell Tools Debug Desktop Window Help

```
59 -  TgtPanel = uipanel( 'Parent', GUIfig, ...
60        'Tag', 'TgtPanel', ...
61        'Units', 'pixel', ...
62        'Position', [30 180 250 150], ...
63        'ForegroundColor', [0.251 0 0.251], ...
64        'Title', 'Target Parameters');
65    % ---------- Objects in Target Panel -----------------
66    %   XT0 Value
67 -  uicontrol(  'Parent', TgtPanel, ...
68        'Tag', 'XTval', ...
69        'Style', 'edit', ...
70        'Units', 'pixels', ...
71        'Position', [20 100 70 20], ...
72        'BackgroundColor', [1 1 1], ...
73        'String', appData.XT0, ...
74        'Callback', @XTval_Callback);
75 -  uicontrol(  'Parent', TgtPanel, ...
76        'Tag', 'XTvalTXT', ...
77        'Style', 'text', ...
78        'Units', 'pixels', ...
79        'Position', [40 80 30 20], ...
80        'String', 'XT0');
81    %   YT0 Value
82 -  uicontrol(  'Parent', TgtPanel, ...
83        'Tag', 'YTval', ...
84        'Style', 'edit', ...
85        'Units', 'pixels', ...
86        'Position', [160 100 70 20], ...
87        'BackgroundColor', [1 1 1], ...
```

TwoD_EngageGUI Ln 71 Col 36 OVR

Figure A11. MATLAB Code (continued)

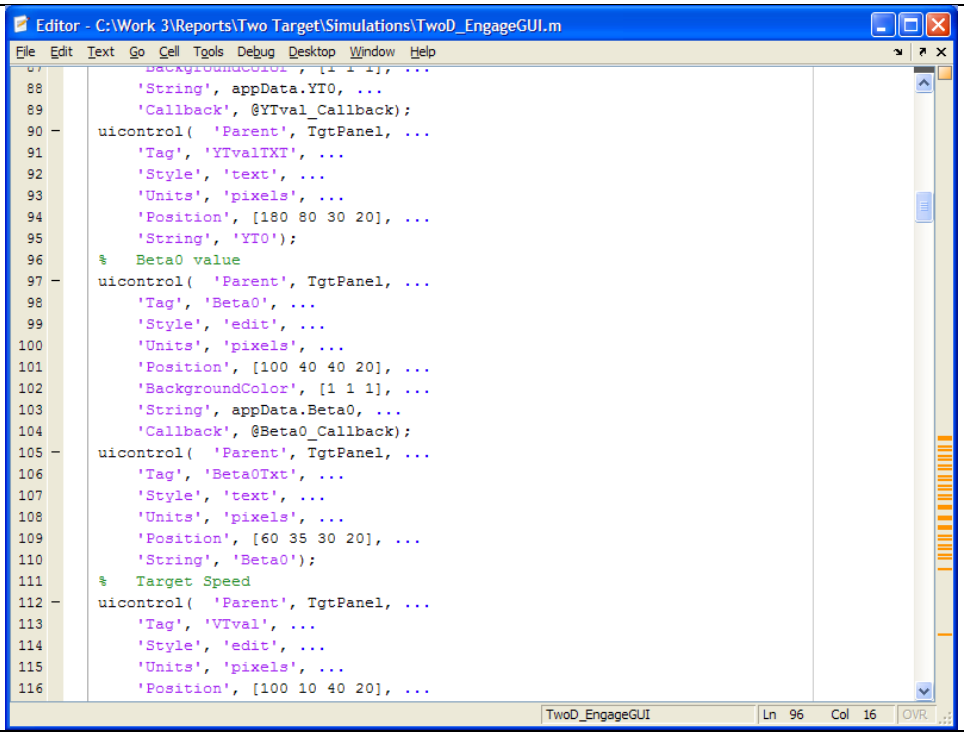

Figure A12. MATLAB Code (continued)

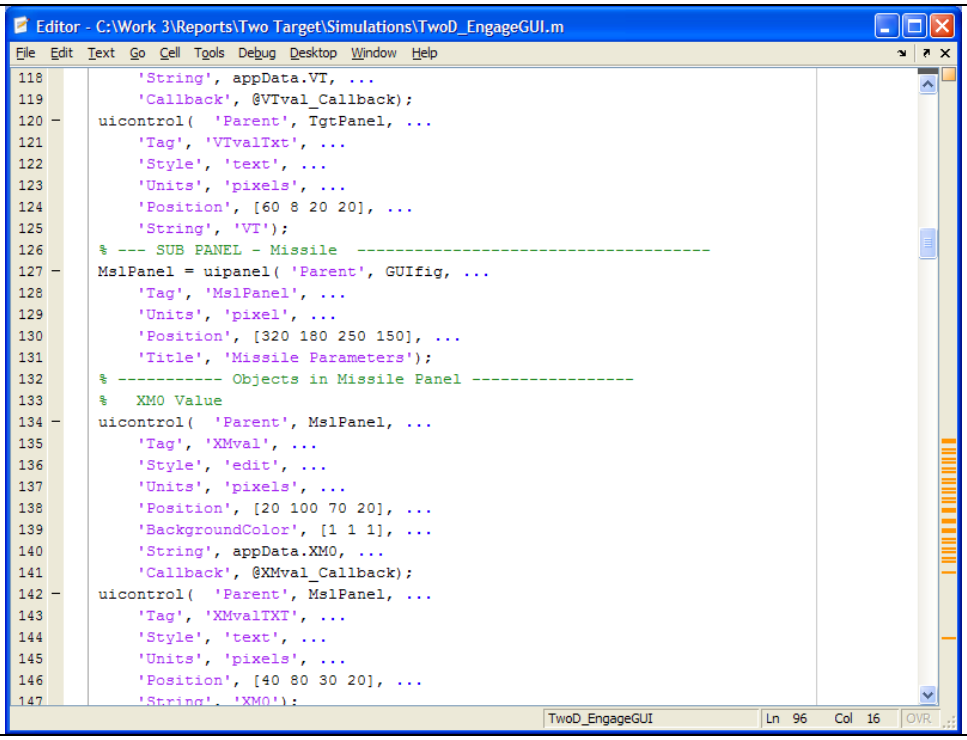

Figure A13. MATLAB Code (continued)

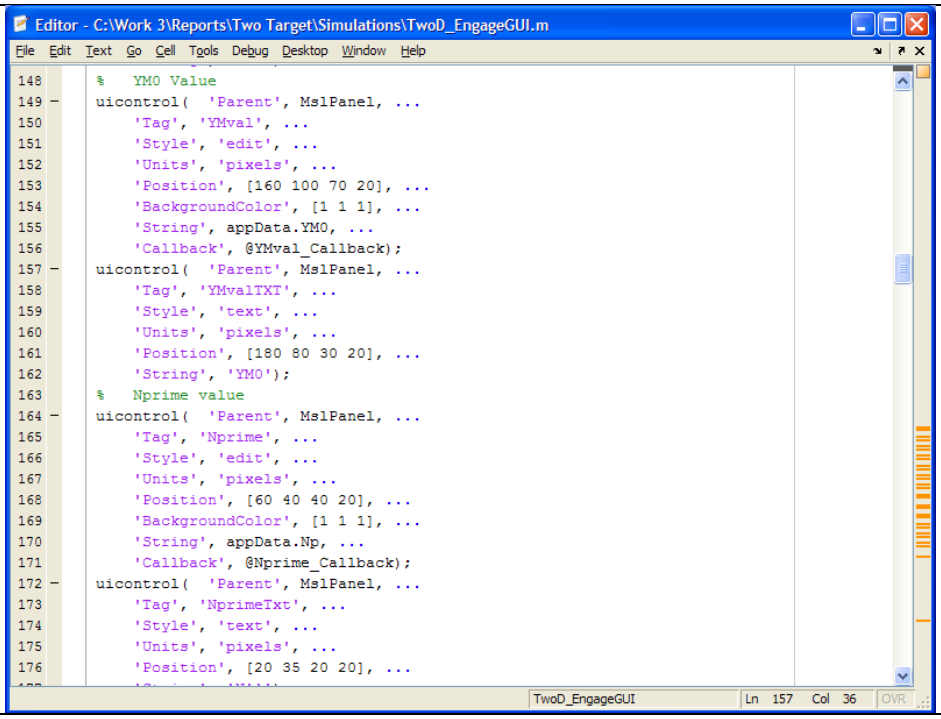

Figure A14. MATLAB Code (continued)

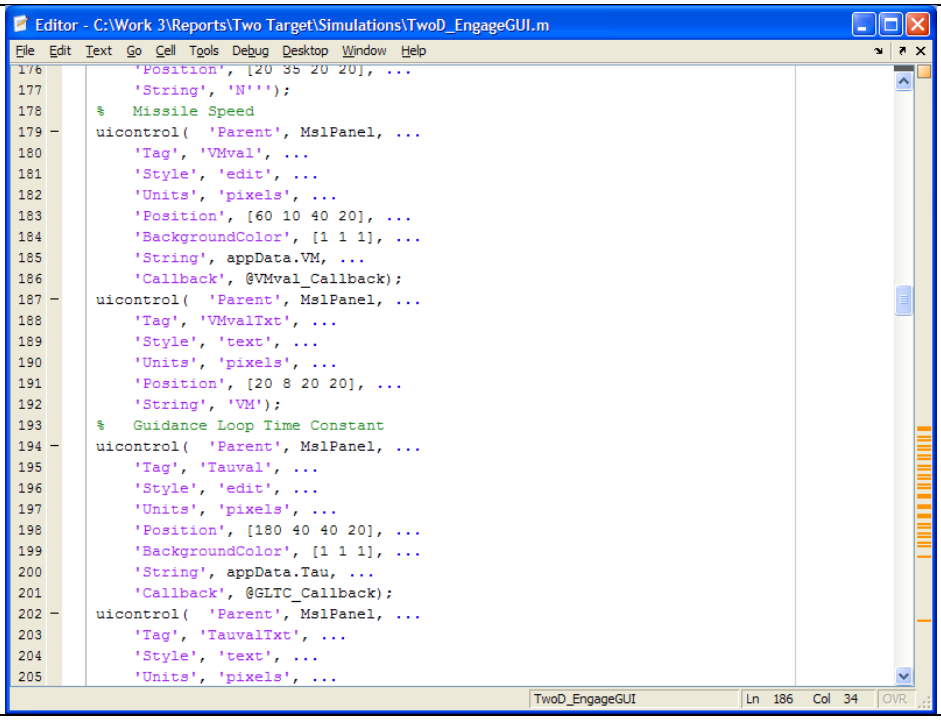

Figure A15. MATLAB Code (continued)

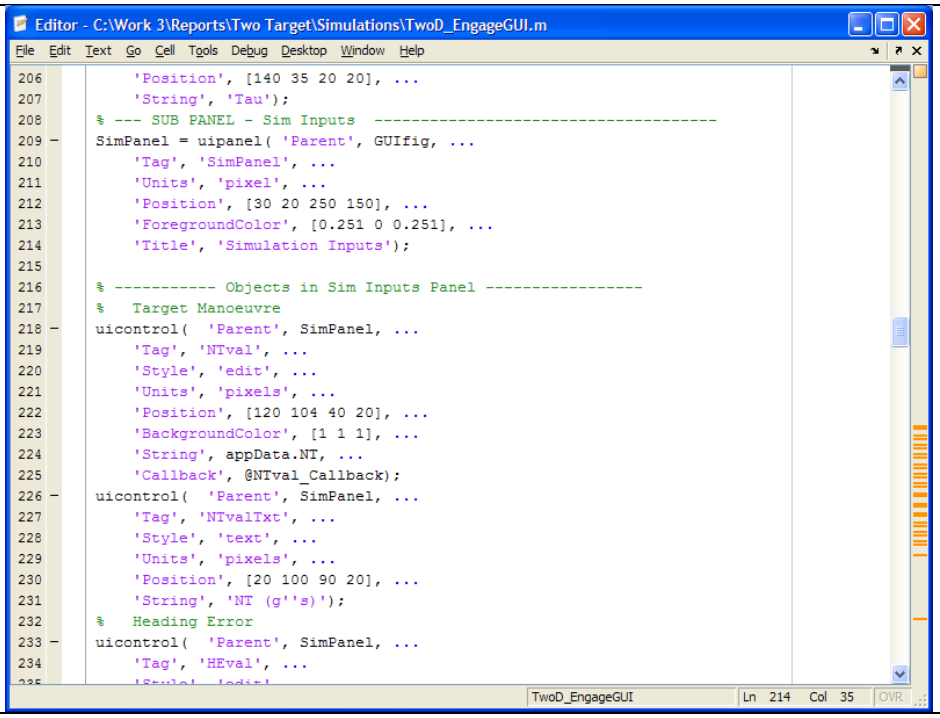

Figure A16. MATLAB Code (continued)

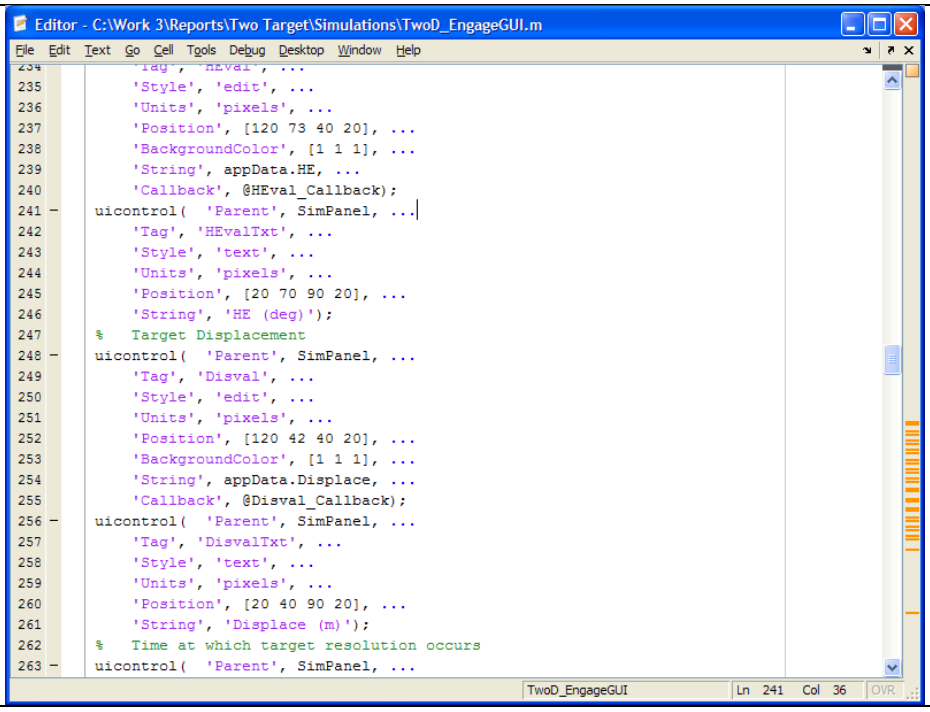

Figure A17. MATLAB Code (continued)

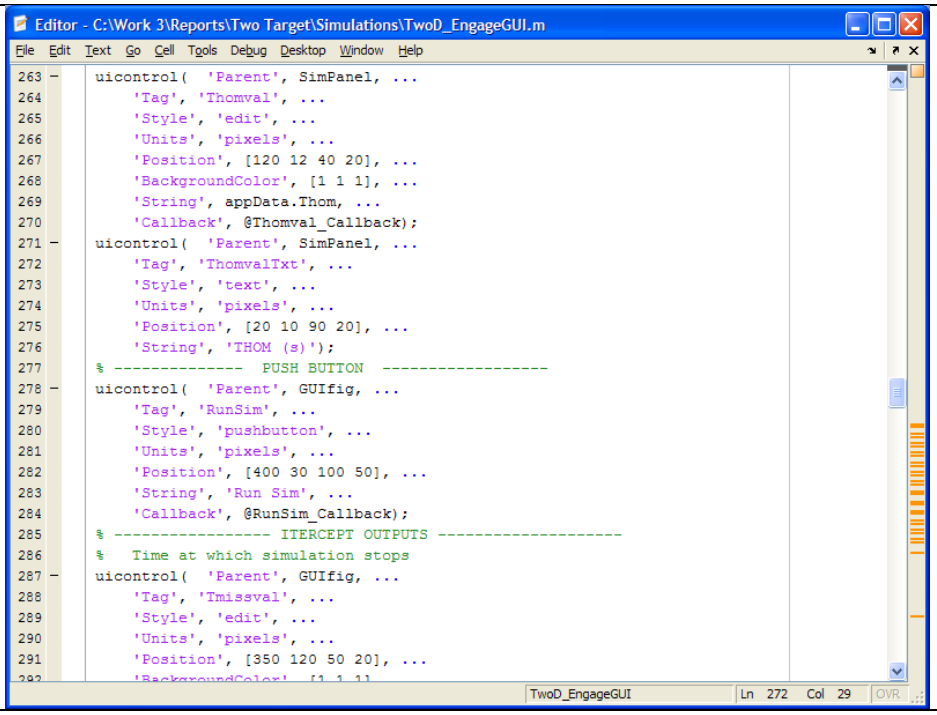

Figure A18. MATLAB Code (continued)

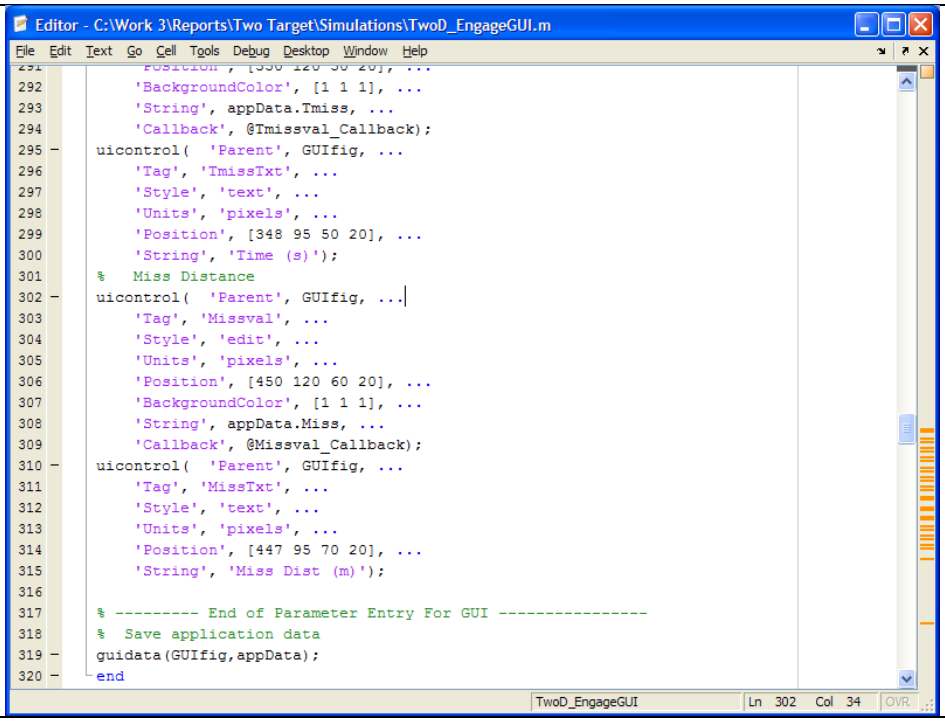

Figure A19. MATLAB Code (continued)

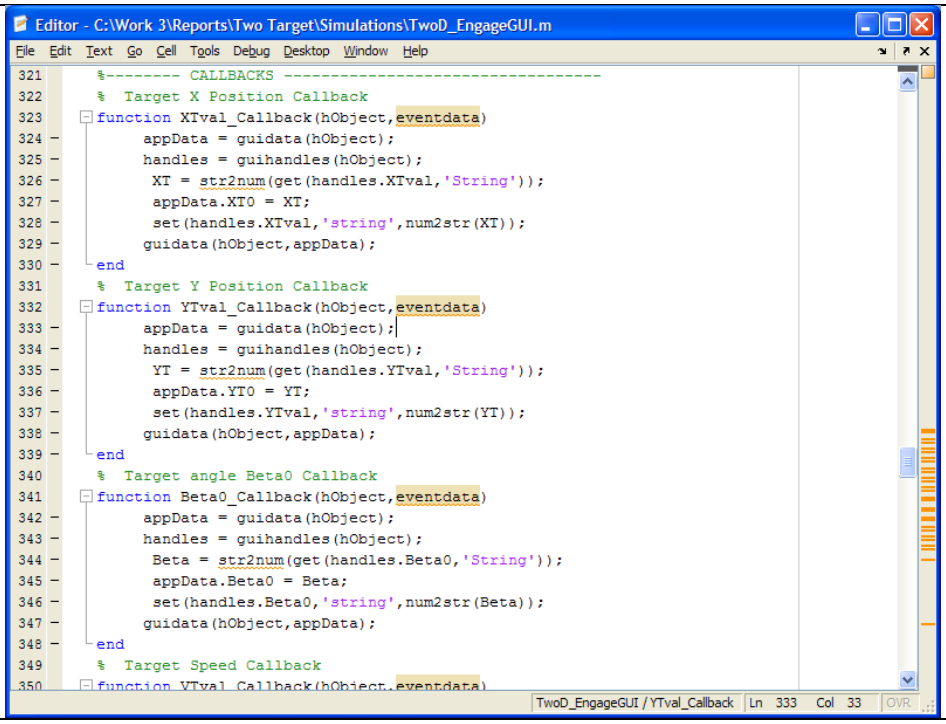

Figure A20. MATLAB Code (continued)

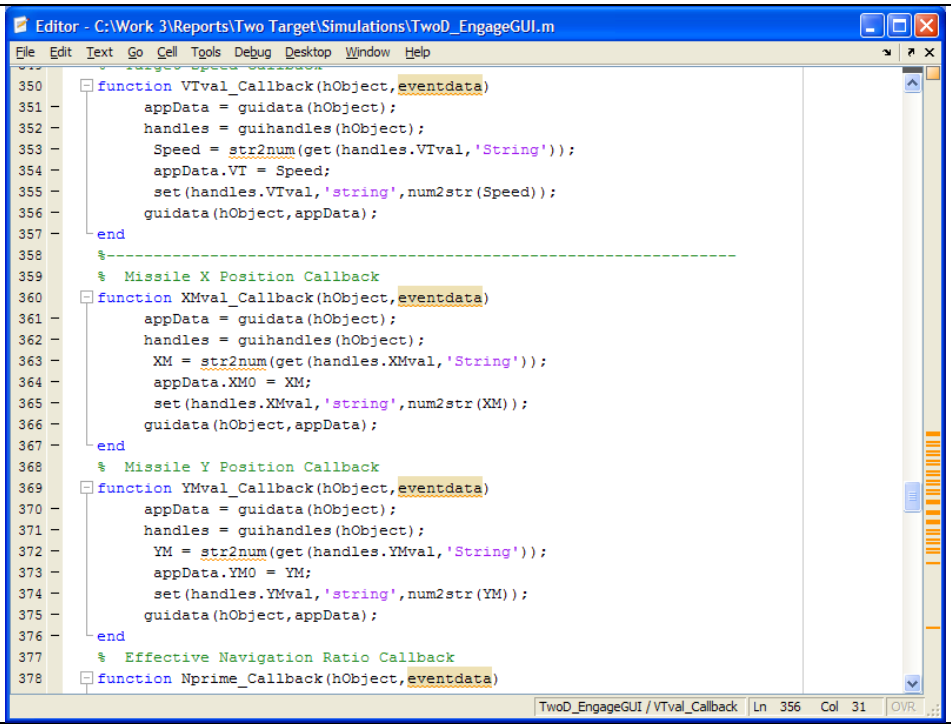

Figure A21. MATLAB Code (continued)

Editor - C:\Work 3\Reports\Two Target\Simulations\TwoD_EngageGUI.m

File Edit Text Go Cell Tools Debug Desktop Window Help

```
function Nprime_Callback(hObject,eventdata)
      appData = guidata(hObject);
      handles = guihandles(hObject);
       Nav = str2num(get(handles.Nprime,'String'));
       appData.Np = Nav;
       set(handles.Nprime,'string',num2str(Nav));
      guidata(hObject,appData);
end
 %  Missile Speed Callback
function VMval_Callback(hObject,eventdata)
      appData = guidata(hObject);
      handles = guihandles(hObject);
       Speed = str2num(get(handles.VMval,'String'));
       appData.VM = Speed;
       set(handles.VMval,'string',num2str(Speed));
      guidata(hObject,appData);
end
 %--------------------------------------------------------------------------
 %  Target Manoeuvre Callback
function NTval_Callback(hObject,eventdata)
      appData = guidata(hObject);
      handles = guihandles(hObject);
       TM = str2num(get(handles.NTval,'String'));
       appData.NT = TM;
       set(handles.NTval,'string',num2str(TM));
      guidata(hObject,appData);
end
 %  Heading Error Callback
function HEval_Callback(hObject,eventdata)
      appData = guidata(hObject);
```

TwoD_EngageGUI / VMval_Callback Ln 391 Col 26 OVR

Figure A22. MATLAB Code (continued)

Editor - C:\Work 3\Reports\Two Target\Simulations\TwoD_EngageGUI.m

File Edit Text Go Cell Tools Debug Desktop Window Help

```
      appData = guidata(hObject);
      handles = guihandles(hObject);
       HdgErr = str2num(get(handles.HEval,'String'));
       appData.HE = HdgErr;
       set(handles.HEval,'string',num2str(HdgErr));
      guidata(hObject,appData);
end
 %  Target Displacement Callback
function Disval_Callback(hObject,eventdata)
      appData = guidata(hObject);
      handles = guihandles(hObject);
       Disp = str2num(get(handles.Disval,'String'));
       appData.Displace = Disp;
       set(handles.Disval,'string',num2str(Disp));
      guidata(hObject,appData);
end
 %  Homing Time Callback
function Thomval_Callback(hObject,eventdata)
      appData = guidata(hObject);
      handles = guihandles(hObject);
       Thom = str2num(get(handles.Thomval,'String'));
       appData.Thom = Thom;
       set(handles.Thomval,'string',num2str(Thom));
      guidata(hObject,appData);
end
 %  Guidance Loop Time Constant Callback
function GLTC_Callback(hObject,eventdata)
      appData = guidata(hObject);
      handles = guihandles(hObject);
```

TwoD_EngageGUI / Disval_Callback Ln 422 Col 4 OVR

Figure A23. MATLAB Code (continued)

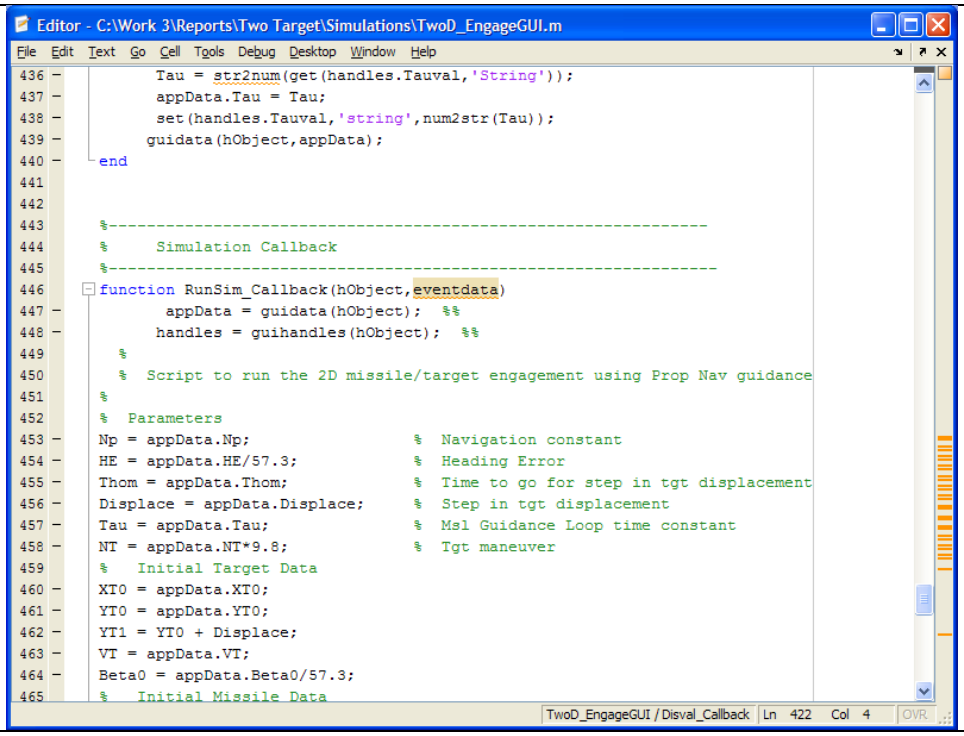

Figure A24. MATLAB Code (continued)

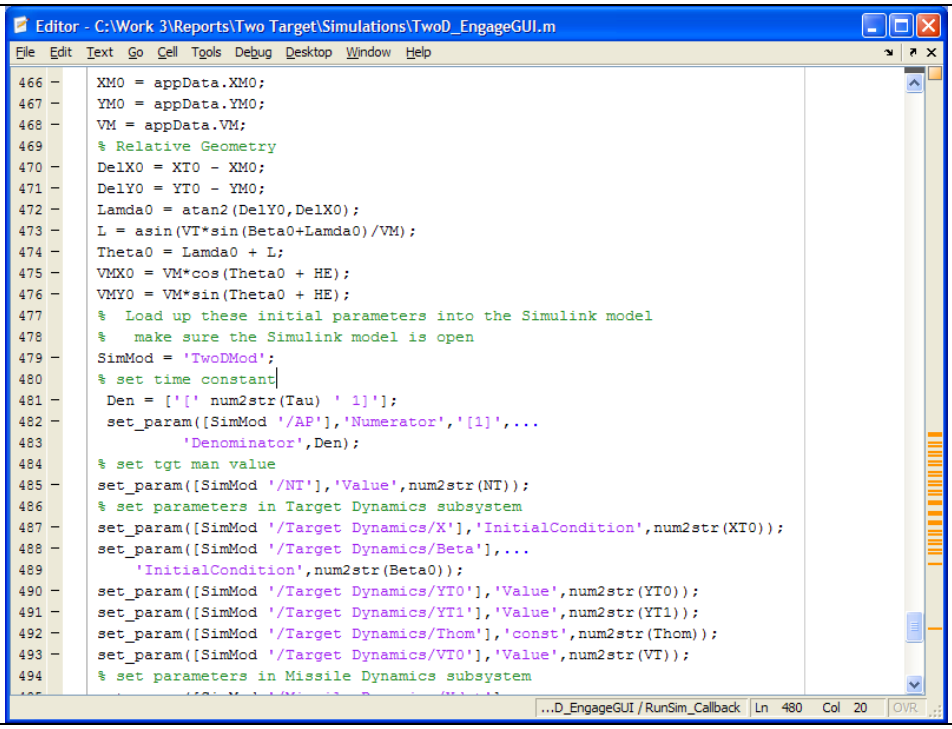

Figure A25. MATLAB Code (continued)

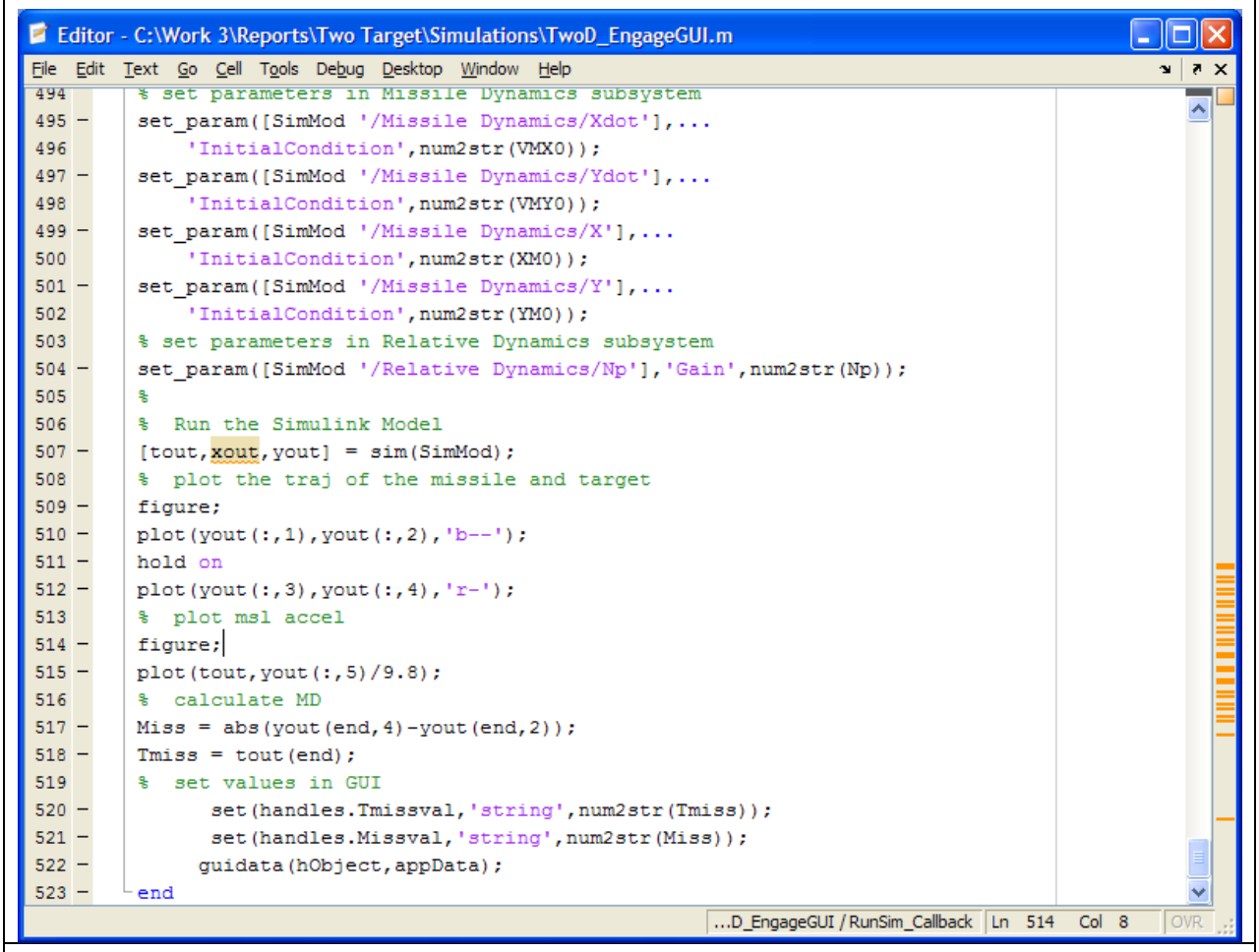

Figure A26. MATLAB Code (continued)

Appendix B: Closed Form Solutions for Single Time Constant Guidance System

If the guidance system can be approximated by a single time constant parameter with transfer function of the form, (see equation (25) in the text)

$$W(s) = \frac{N'}{s(1+\tau s)}, \tag{B1}$$

then, for integral values of N', it has been shown in the text how to derive useful closed form solutions to the linear engagement problem. In particular, typical closed form solutions have been provided therein for the specific case when $N' = 3$. These analytical expressions are useful when producing design curves during the preliminary stages of a guided missile program. In this appendix, closed form solutions for integral values of N' in the range [4 – 6] are provided.

B.1. Solution for N′ = 4

$$\left.\frac{MD_{NT}}{n_T}\right|_{N'=4} = \frac{t_F^2}{2} e^{-t_F/\tau}\left[1 - \frac{t_F}{3\tau}\right], \tag{B2}$$

$$\left.\frac{MD_{HA}}{HE}\right|_{N'=4} = -V_M t_F e^{-t_F/\tau}\left[1 - \frac{t_F}{\tau} + \frac{t_F^2}{6\tau^2}\right], \tag{B3}$$

$$\left.\frac{MD_{YT}}{YT}\right|_{N'=4} = e^{-t_F/\tau}\left[1 - \frac{t_F}{\tau} + \frac{t_F^2}{6\tau^2}\right], \tag{B4}$$

B.2. Solution for N′ = 5

$$\left.\frac{MD_{NT}}{n_T}\right|_{N'=5} = \frac{t_F^2}{2} e^{-t_F/\tau}\left[1 - \frac{2t_F}{3\tau} + \frac{t_F^2}{12\tau^2}\right], \tag{B5}$$

$$\left.\frac{MD_{HA}}{HE}\right|_{N'=5} = -V_M t_F e^{-t_F/\tau}\left[1-\frac{3t_F}{2\tau}+\frac{t_F^2}{2\tau^2}-\frac{t_F^3}{24\tau^3}\right] \quad , \tag{B6}$$

$$\left.\frac{MD_{YT}}{YT}\right|_{N'=5} = e^{-t_F/\tau}\left[1-\frac{3t_F}{2\tau}+\frac{t_F^2}{2\tau^2}-\frac{t_F^3}{24\tau^3}\right] \quad , \tag{B7}$$

B.3. Solution for N′ = 6

$$\left.\frac{MD_{NT}}{n_T}\right|_{N'=6} = \frac{t_F^2}{2}e^{-t_F/\tau}\left[1-\frac{t_F}{\tau}+\frac{t_F^2}{4\tau^2}-\frac{t_F^3}{60\tau^3}\right] \quad , \tag{B8}$$

$$\left.\frac{MD_{HA}}{HE}\right|_{N'=6} = -V_M t_F e^{-t_F/\tau}\left[1-\frac{2t_F}{\tau}+\frac{t_F^2}{\tau^2}-\frac{t_F^3}{6\tau^3}+\frac{t_F^4}{120\tau^4}\right] \quad , \tag{B9}$$

$$\left.\frac{MD_{YT}}{YT}\right|_{N'=6} = e^{-t_F/\tau}\left[1-\frac{2t_F}{\tau}+\frac{t_F^2}{\tau^2}-\frac{t_F^3}{6\tau^3}+\frac{t_F^4}{120\tau^4}\right] \quad , \tag{B10}$$

The above closed form solutions have been verified against the Simulink models.

It is interesting to note from the above expressions that the miss distance due to a target displacement appears to be directly related to the miss distance due to a heading error in the following way,

$$\left.\frac{MD_{YT}}{YT}\right|_{N'=n} = \frac{1}{t_F}\left.\frac{MD_{HA}}{(-V_M HE)}\right|_{N'=n} , \tag{B11}$$

where n is an integer greater than 2. In fact, through simulation of the adjoint models in Simulink, it was straightforward to verify that this relationship holds true even for non-integer values of N' and also for higher order systems such as the fifth order binomial system. Further investigations of this relationship are carried out in Appendix C.

Appendix C: Alternative Approach to Performance Prediction of Miss Distance due to a Step in Target Displacement

The relationship given in equation (B11) expresses the fact that the miss distance due to a step in target displacement, for a single time constant system, may be determined by knowing the miss distance due to an initial error in heading angle. That is, imposing an initial heading angle on the interceptor of the form

$$HA = \frac{YT}{t_F}, \tag{C1}$$

and assuming there are no other inputs to the system, then the miss distance output for the problem is that due to a step in target displacement of magnitude YT. This is certainly true of the closed form solutions given in the main text and in Appendix B above. The investigation here will focus on whether this is true for non-integral values of N' and also for higher order guidance systems.

Let the initial heading angle condition, equivalent to equation (C1) above, be denoted by HA_{YT}. Imposing this condition on the first integrator in Figure C1 is tantamount to imposing a step, of magnitude YT, in target displacement condition on the second integrator in the diagram.

C.1. Linear System Investigations

For the linear analysis, either Model A or Model B may be used in this case as they have been shown to produce equivalent results when the input is heading error. For the present investigation, Model A is employed. The Model A forward loop block diagram incorporating the HA_{YT} initial condition, as expressed in equation (C1), is presented in Figure C1.

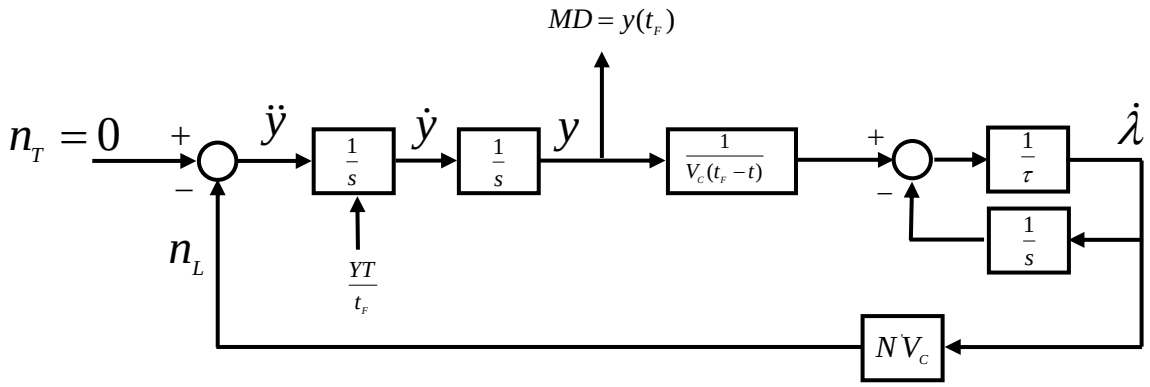

Figure C1: Model A with HA_{YT} condition

The adjoint model of Figure C1 may be easily constructed using the adjoint construction rules and is displayed in Figure C2.

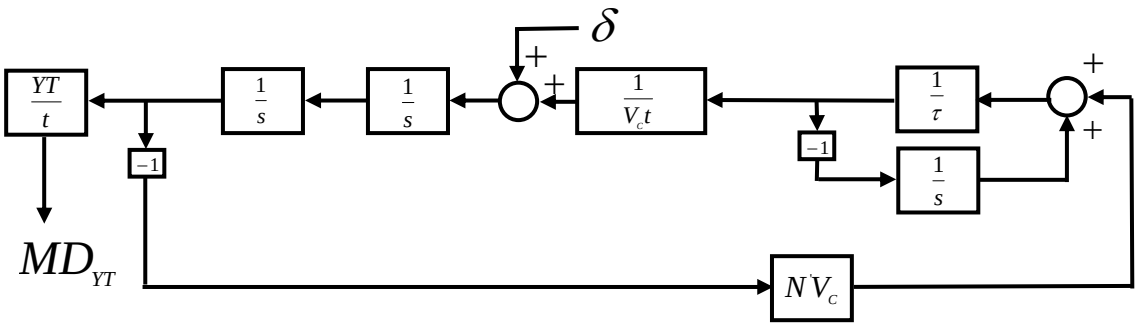

Figure C2: Adjoint of Model A with HA_{YT} condition

The adjoint model is employed here because of the desire to compare the miss distance profiles in only one run. The Simulink representation of the adjoint block diagram for carrying out the adjoint simulation is shown in Figure C3 below.

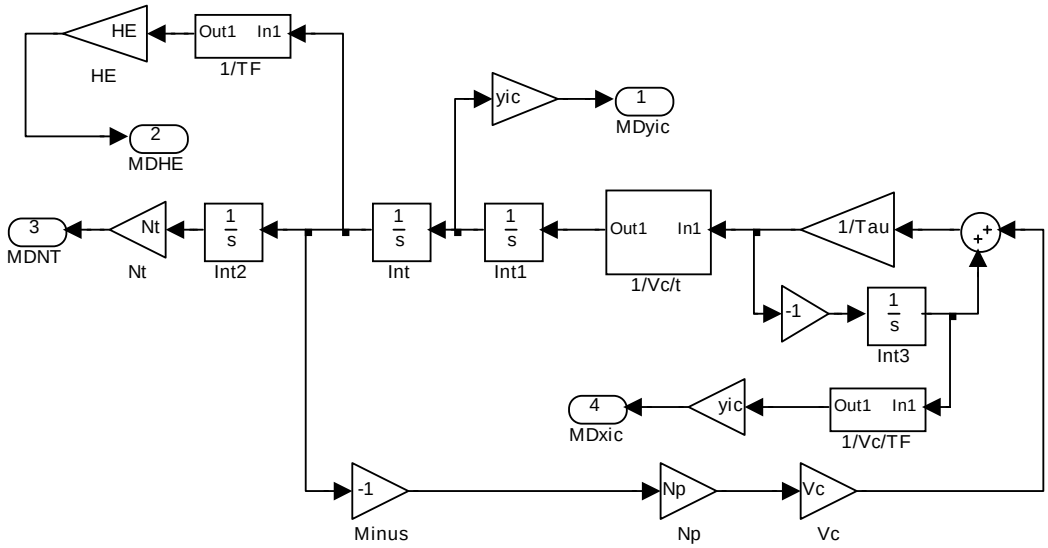

Figure C3: Simulink Representation of Adjoint Model A

In this case, output channels 1, 2 and 4 shown in Figure C3 are of interest. Output channels 1 and 4 provide the data to compute the miss distance response to a step in target displacement

of magnitude YT=yic while output channel 2 provides the data for the same response via the indirect approach proposed here using the HA_{YT} condition.

The miss distance results generated for the case of a single time constant system are compared in Figure C4. For selected values of the navigation ratio, the plots compare the miss distance due to a target displacement (YT=yic) derived using the conventional approach with that using the HA_{YT} approach. It is clear from the figure that the results agree even if the value of N' is non-integral. In Figure C5, simulation results generated on the basis of a fifth order guidance system are presented. Again, the HA_{YT} approach is seen to agree favourably with the conventional approach to the miss distance problem for this case.

In conclusion, for a linear guidance system, the miss distance performance due to a step in target displacement may be determined on the basis of an appropriate heading error input thus eliminating the need to model the target displacement effect conventionally. This approach also obviates the need to incorporate the correction factor in Model A as outlined earlier in the text.

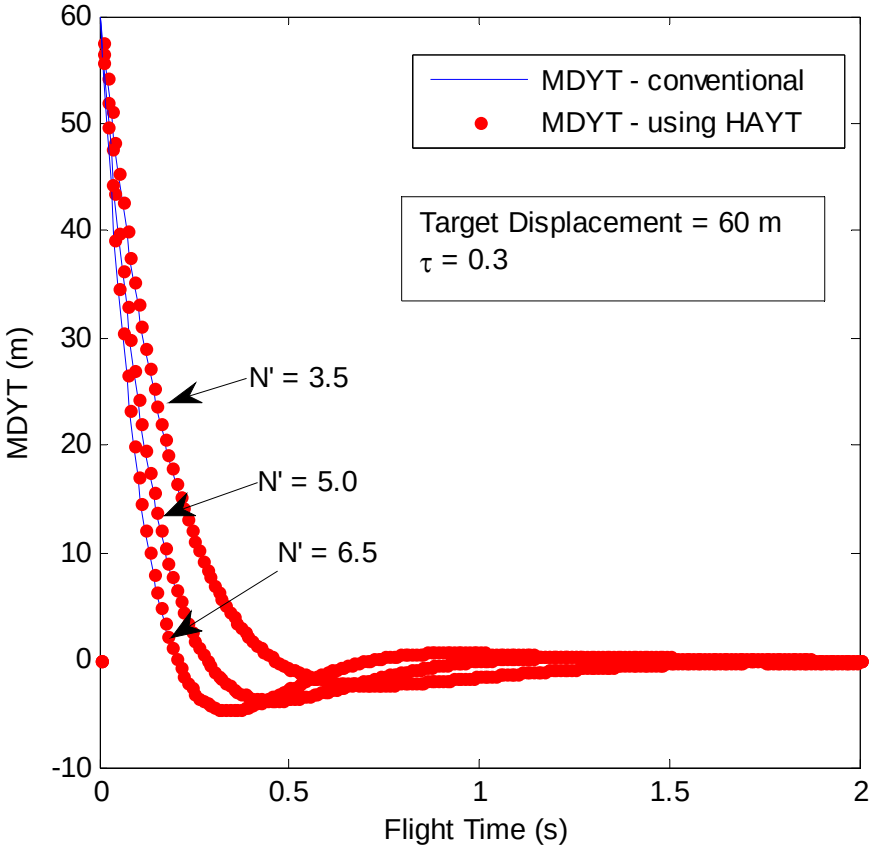

Figure C4: Comparison of HA_{YT} approach with direct approach for single time constant system

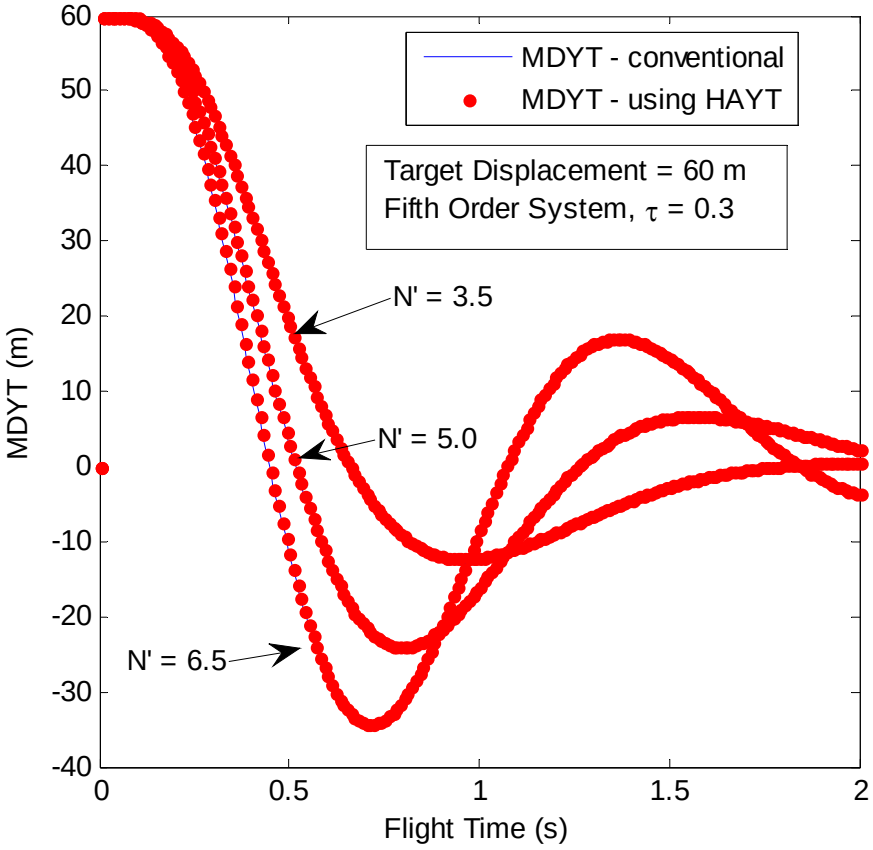

Figure C5: Comparison of HA_{YT} approach with direct approach for fifth order system

C.2. Non-linear System Investigations

In this section, the accuracy of the HA_{YT} approach is investigated in the context of the non-linear simulation model. Figure C6 shows the typical trajectories involved when implementing either the conventional approach or the HA_{YT} approach. As stated earlier, the conventional approach here means applying the target displacement initial condition at a certain time to go before intercept while the HA_{YT} approach means applying an equivalent initial condition in accordance with equation (C1). In order to implement the HA_{YT} condition, it is necessary to estimate the intercept time at the start of the simulation. In this regard, the following approximation is utilised, namely, $t_F = R/V_C$. In Figure C7 is presented the miss distance profile generated by carrying out multiple runs of the non-linear simulation model employing the HA_{YT} initial condition. All other inputs are set to zero in this case. Superimposed on this plot is the corresponding miss distance profile produced by the linear model. The results agree favourably.

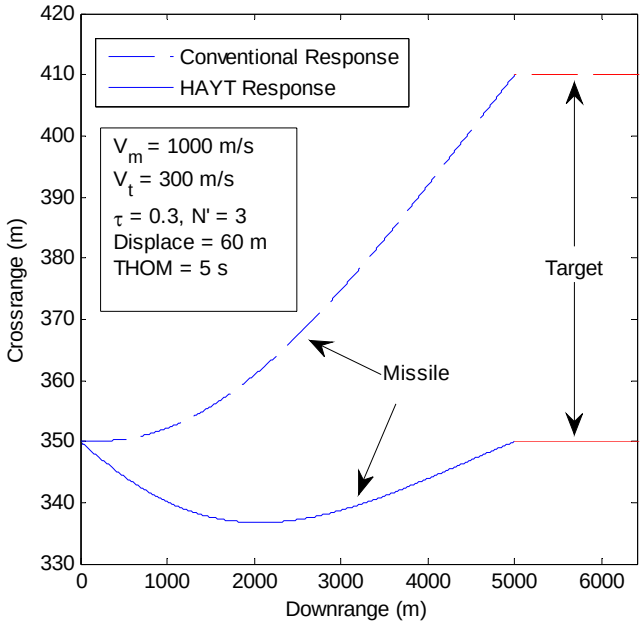

Figure C6: Comparison of Conventional and HA_{YT} based Trajectories

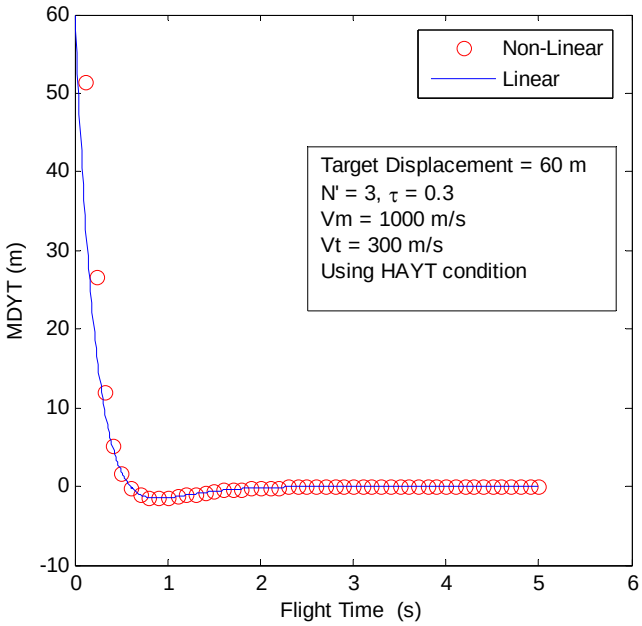

Figure C7: Comparison of Linear and Non-linear Results using the HA_{YT} Condition

Next, the comparison of the HA_{YT} based results with those generated using the conventional approach is made, using the non-linear model outlined in Section 2 in the text. All inputs

except the initial target displacement are set to zero in this case. The simulation results are shown in Figure C8 below.

The non-linear simulations are repeated in order to examine the effects on the miss distance results due to other input conditions, such as target manoeuvre and heading error. The total miss distance results are shown in Figure C9 below. Note that these results are based on a target displacement of 60 m.

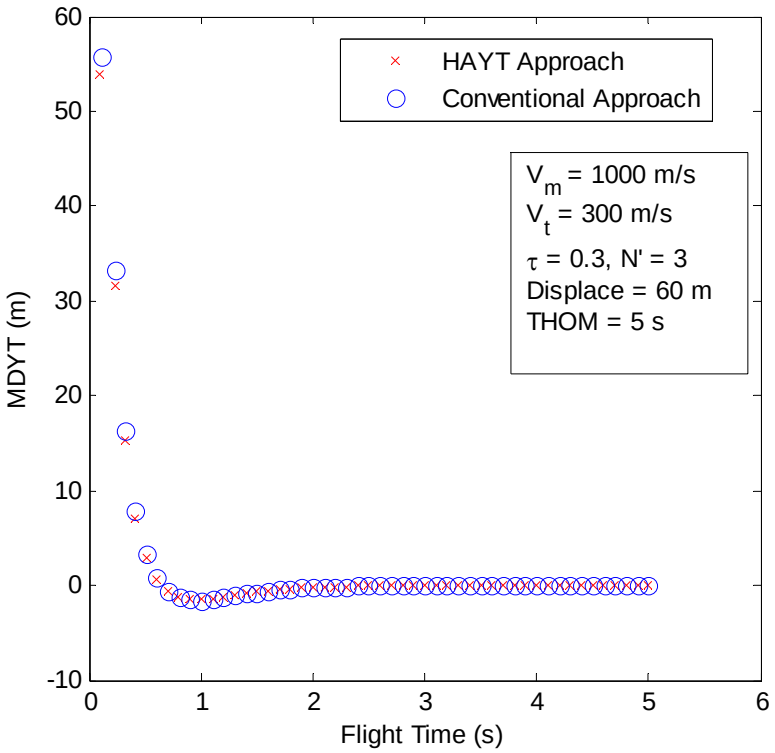

Figure C8: Non-linear Results Comparing Conventional and HA_{YT} Approach (Single Input)

Finally, using the non-linear simulation model, the effect of different target displacements on the total miss distance results is investigated. The plots are summarised in Figure C10 and compare the miss distance profiles generated using the conventional approach with those generated using the HA_{YT} approach. It is clear from the plots that the proposed HA_{YT} approach to the target displacement problem leads to acceptable results in this case. Moreover, for flight times larger than 1 second, the plots indicate that the PN guidance law works well in eliminating errors due to the initial target displacement and therefore the miss distance is insensitive to the magnitude of the initial target displacement. However, if the homing time is less than 1 second, the miss distance only reduces as the magnitude of initial target displacement is reduced.

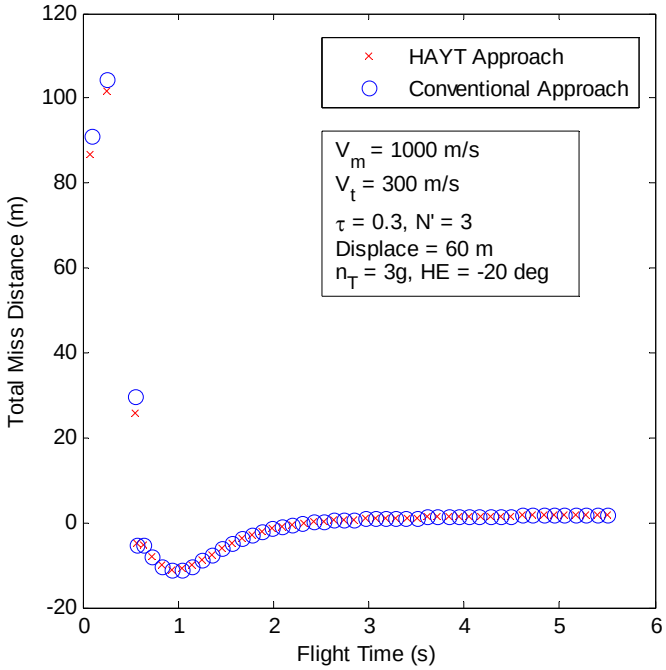

Figure C9: Non-linear Results Comparing Conventional and HA$_{YT}$ Approach (Multiple Inputs)

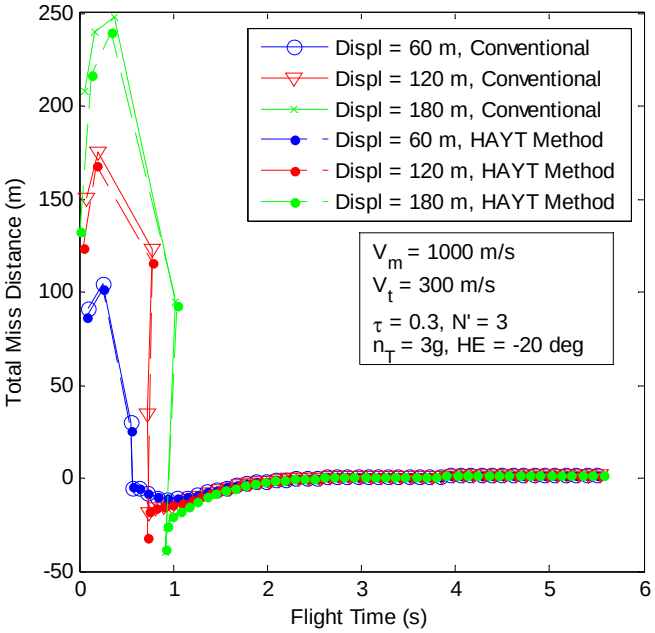

Figure C10: Comparison of HA$_{YT}$ Method with Conventional Method

DEFENCE SCIENCE AND TECHNOLOGY ORGANISATION
DOCUMENT CONTROL DATA

1. PRIVACY MARKING/CAVEAT (OF DOCUMENT)

2. TITLE

On Alternative Formulations for Linearised Miss Distance Analysis

3. SECURITY CLASSIFICATION (FOR UNCLASSIFIED REPORTS THAT ARE LIMITED RELEASE USE (L) NEXT TO DOCUMENT CLASSIFICATION)

Document	(U)
Title	(U)
Abstract	(U)

4. AUTHOR(S)

Domenic Bucco and Rick Gorecki

5. CORPORATE AUTHOR

DSTO Defence Science and Technology Organisation
PO Box 1500
Edinburgh South Australia 5111 Australia

6a. DSTO NUMBER	6b. AR NUMBER	6c. TYPE OF REPORT	7. DOCUMENT DATE
DSTO-TR-2845	AR-015-622	Technical Report	May 2013

8. FILE NUMBER	9. TASK NUMBER	10. TASK SPONSOR	11. NO. OF PAGES	12. NO. OF REFERENCES
2011/1280453/1	DERP 07/372	DSTO	67	6

DSTO Publications Repository

http://dspace.dsto.defence.gov.au/dspace/

14. RELEASE AUTHORITY

Chief, Weapons Systems Division

15. SECONDARY RELEASE STATEMENT OF THIS DOCUMENT

Approved for public release

OVERSEAS ENQUIRIES OUTSIDE STATED LIMITATIONS SHOULD BE REFERRED THROUGH DOCUMENT EXCHANGE, PO BOX 1500, EDINBURGH, SA 5111

16. DELIBERATE ANNOUNCEMENT

No Limitations

17. CITATION IN OTHER DOCUMENTS Yes

18. DSTO RESEARCH LIBRARY THESAURUS

intercept guidance, miss distance, analysis and simulation, homing loop, adjoint

19. ABSTRACT

In this report, techniques generally employed in the analysis of intercept guidance problems are reviewed. From the governing non-linear equations describing such problems, two basic linear models are derived. Traditionally, these linear models are utilised as a basis for preliminary intercept engagement studies. Under certain input conditions, the two models are mathematically equivalent and, hence, have been used interchangeably by weapons analysts to yield appropriate design and performance data in support of their programs. However, for a specific set of initial conditions, which includes a very important class of practical problems that may be assessed with the use of these models, it is noted herein that one of these linear models produces incorrect performance data when compared to a non-linear simulation of the engagement. In contrast, the other model produces consistent results with those generated by the non-linear simulation regardless of the initial conditions considered. To remedy this discrepancy, the necessary mathematics are derived to bring the two formulations into alignment for any form of the initial conditions and inputs to the system. Consequently, this leads to a consistency in the corresponding adjoint models which are constructed from these linear models, thus ensuring the generation of correct output data regardless of which model is employed by the analyst.